JACS
JOURNAL OF THE AMERICAN CHEMICAL SOCIETY

Open Access
This article is licensed under CC-BY-NC-ND 4.0

pubs.acs.org/JACS
Article

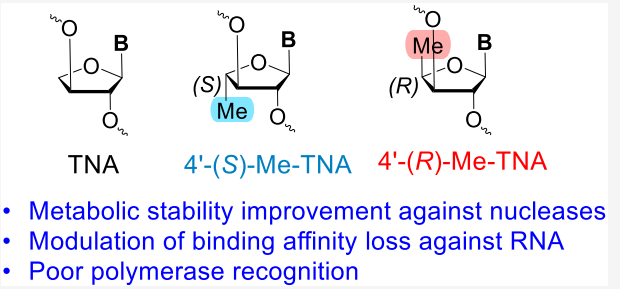
Chiral-4′-Methyl-α-(L)-Threofuranosyl Nucleic Acids: Synthesis, Structure, Binding Affinity, Nuclease Resistance, and Polymerase Recognition

Atsushi Mikami, Dhrubajyoti Datta, Jayanta Kundu, Vathan Kumar, Namrata Erande, Esau Medina, Victoria A. Maola, Erica M. Lee, Shigeo Matsuda, Joel M. Harp, Martin Egli, John C. Chaput, and Muthiah Manoharan*

Cite This: J. Am. Chem. Soc. 2026, 148, 38692−38706
Read Online

ACCESS | Metrics & More | Article Recommendations | Supporting Information

ABSTRACT: α-(L)-(3′−2′)-Threofuranosyl nucleic acid (TNA) cross-pairs with DNA and RNA and is not degraded by nucleases and thus has potential for use in diagnostics and therapeutics based on nucleic acids. Here, we describe the synthesis of 15 building blocks of chiral 4′-(*R*)- and 15 building blocks of chiral (*S*)-methyl-α-(L)-threofuranosyl nucleic acid (4′-Me-TNA) monomers and their incorporation into oligonucleotides. Crystallographic studies of RNAs containing 4′-Me-TNA modifications revealed the impact of the methyl substituent on the sugar pucker and duplex conformation. Biostability studies showed that a terminal 4′-Me-TNA modification on a deoxyoligonucleotide imparted resistance to nuclease digestion equivalent to unmethylated TNA, which is markedly superior to that of more conventional 2′-ribo and 2′-deoxy modifications. A single nucleotide incorporation of the 4′-(*R*)-Me-TNA destabilized an otherwise all-RNA 12-mer duplex by 6.5 to 12 °C, depending on the base, relative to the unmodified RNA control duplex; the (*S*) isomer was less destabilizing than the (*R*) isomer. Computational models were used to rationalize the high levels of nuclease resistance and the thermal destabilization. The 4′-Me-TNA triphosphates are poorly recognized by an engineered TNA polymerase making it unlikely that the 4′-Me-TNA triphosphates will be recognized by natural polymerases. Together, these properties warrant the evaluation of 4′-Me-TNA in nucleic acid-based therapeutics.



INTRODUCTION

α-(L)-(3′−2′)-Threofuranosyl nucleic acid (TNA) is an artificial genetic polymer designed and synthesized by Albert Eschenmoser and his colleagues to explore the chemical etiology of RNA.[1] Among the various artificial genetic polymers with aldose sugars that have been synthesized and evaluated experimentally,[2] TNA is the only system that stably and Watson−Crick-specifically base pairs with itself and with complementary strands of DNA and RNA.[1−4] Structural studies revealed that complementary TNA strands form a right-handed antiparallel A-form duplex with a distinctive C4′-exo sugar pucker.[5,6] Due to the backbone repeat unit that is 1 atom shorter than the repeat unit found in DNA and RNA, sequential phosphorus−phosphorus distances are closer for TNA than A- and B-form helices (5.7 vs 6.0 or 6.8 Å, respectively).[6,7] TNA forms more stable duplexes with RNA rather than DNA, since the C4′-exo sugar pucker leads to a helical geometry that is closer in structural space to RNA than DNA.[7] The quasi-diaxial positioning of the phosphates at the 2′ and 3′ hydroxyl positions of the sugar group in TNA leads to a nucleic acid backbone that is refractory to nuclease digestion and resistant to acid-mediated depurination.[8,9] These physicochemical properties have led to

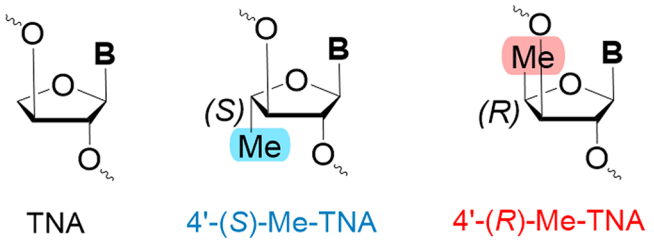


Figure 1. Parent TNA and 4′-(*S*)- and 4′-(*R*)-Me-TNA nucleotides studied in the present work.

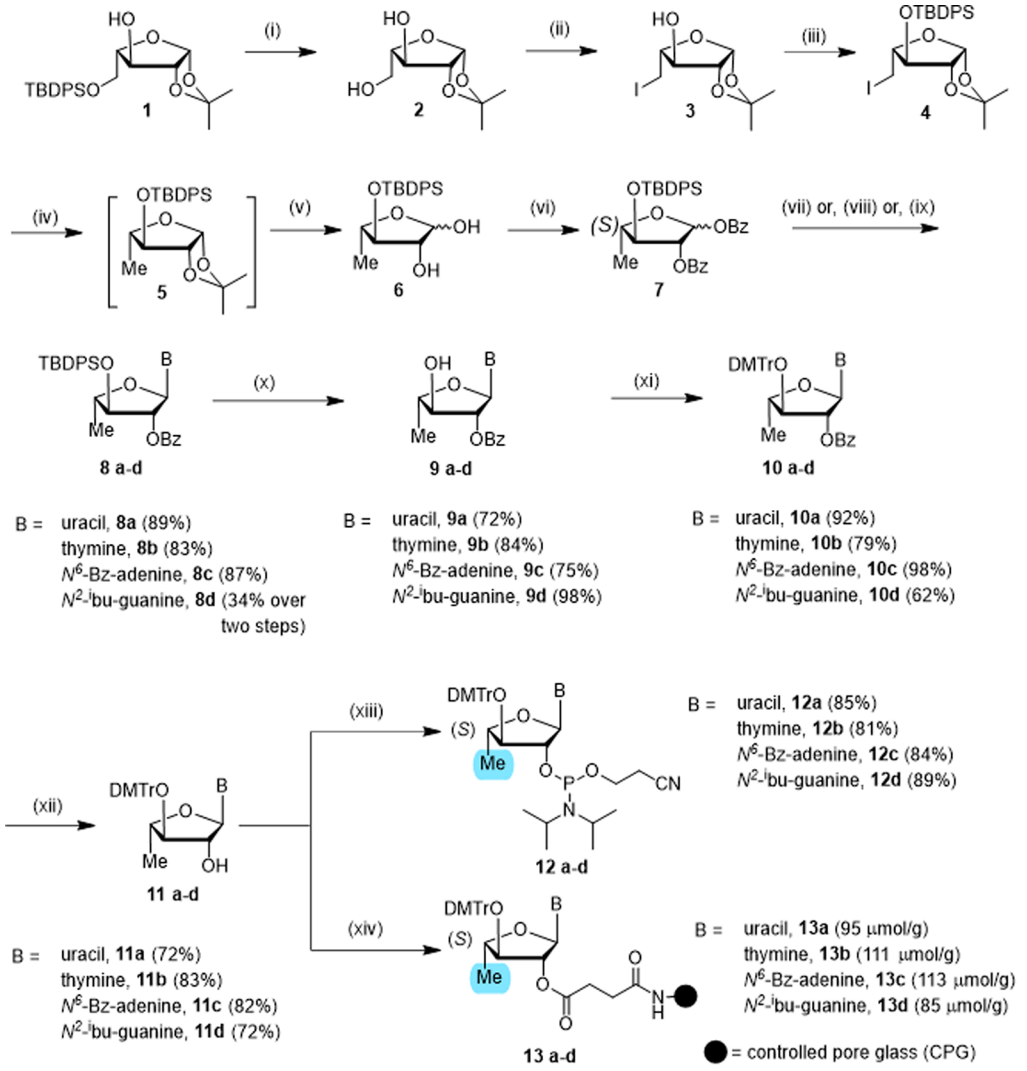
Received: April 5, 2026
Revised: July 20, 2026
Accepted: July 22, 2026
Published: September 2, 2026



ACS Publications
© 2026 The Authors. Published by American Chemical Society

Downloaded from pubs.acs.org/jacsat/article-pdf/148/36/38692/6822318/jacs.6c07051.pdf by VANDERBILT UNIV user on 10 October 2026

Scheme 1. Synthesis of 4′-(*S*)-Me-TNA Sugar Intermediate and Syntheses of 4′-(*S*)-Me-TNA U, T, A, and G Building Blocks[a]



[a]Reagents and conditions: (i) TBAF (1.0 M in THF), THF, 95%; (ii) imidazole, PPh_3, I_2, CH_3CN, 60 °C, 4 h, 94%; (iii) TBDPSCl, imidazole, DMF, room temperature, overnight, 50%; (iv) AIBN, $(TMS)_3SiH$, toluene, 90 °C, 1 h; (v) aqueous TFA (80%), DCM, room temperature, overnight, 46% in two steps; (vi) Bz_2O, 4-dimethylaminopyridine (DMAP), pyridine, room temperature, overnight; (vii) (a) *N*,*O*-bis(trimethylsilyl)acetamide (BSA), CH_3CN, 60 °C, 30 min and (b) TMSOTf, CH_3CN, 60 °C, 2 h for U and T (**8a**,**b**); (viii) (a) BSA, toluene, 90−95 °C, 30 min and (b) TMSOTf, toluene, 90−95 °C, 2 h for N^6-Bz-A (**8c**); (ix) conditions mentioned as (viii) followed by TFA, DCM, 0 °C, 2 h for N^2-ibu-G (**8d**); (x) TBAF (1.0 M in THF), THF, 0 °C, 2 h; (xi) DMT-Cl, $AgNO_3$, THF-pyridine (4:1), room temperature, overnight; (xii) aq. NaOH (1.0 M), THF-MeOH (1:1), room temperature, 3 h; (xiii) 2-cyanoethyl-*N*,*N*-diisopropylchlorophosphoramidite, *N*-methylimidazole (NMI), diisopropylethylamine (DIPEA), DCM, room temperature, 30 min; (xiv) (a) succinic anhydride, DMAP, DCM, room temperature, overnight, (b) LCAA-CPG, DIPEA, HBTU, DMF, mechanical shaker, overnight, and (c) Ac_2O, pyridine, mechanical shaker, room temperature, 3 h.

the evaluation of TNA in diagnostic and therapeutic applications.[10,11]

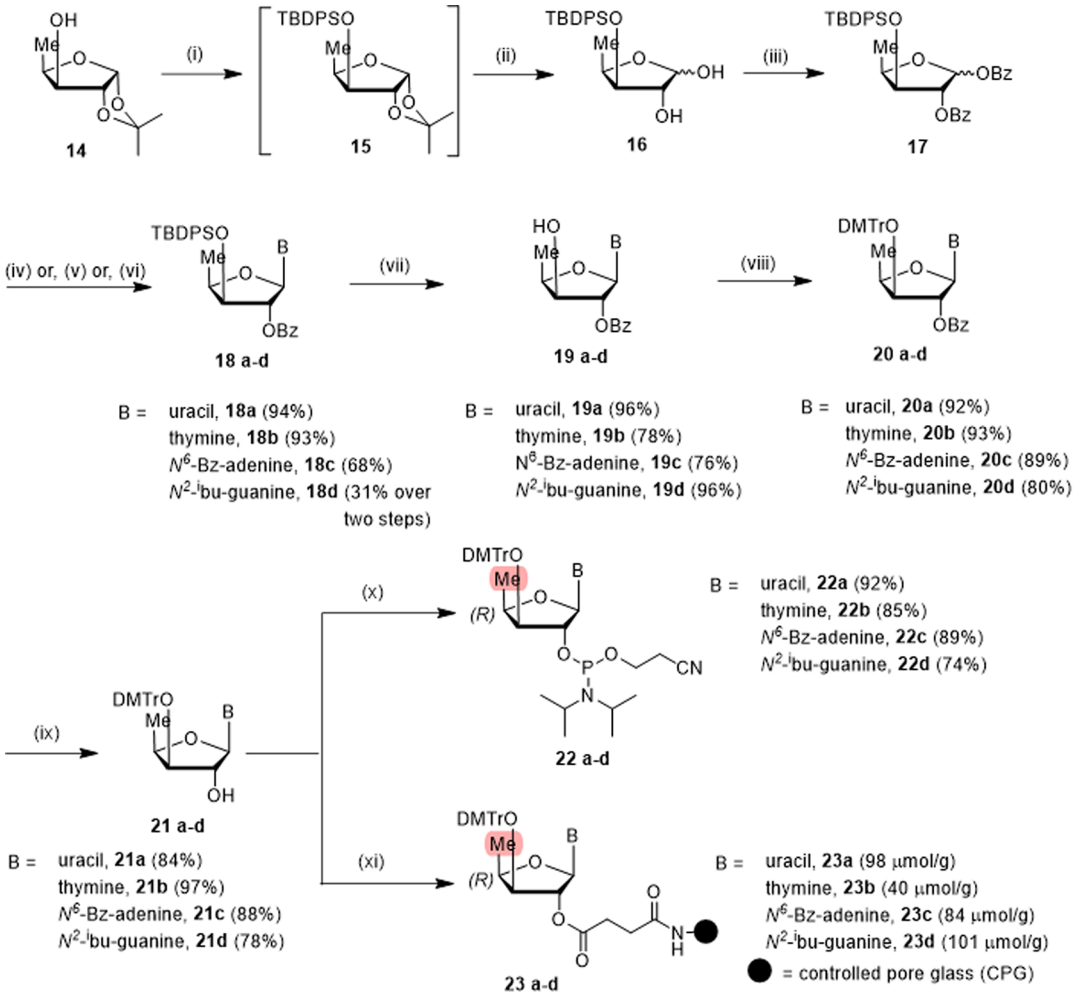
We have previously evaluated the effect of incorporation of TNA into small interfering RNAs (siRNAs), which mediate RNA interference (RNAi).[12] In cultured mammalian cells and in mice, siRNAs containing TNA modifications at certain positions had increased potency, specificity, off-target mitigation, and safety compared to siRNAs lacking the TNA modification.[12] Similarly, antisense oligonucleotides containing TNA showed potent activity with low toxicity.[13] TNA oligomers that bind specifically to certain ligands[14,15] and that have catalytic activity[16] have been identified by in vitro selection using engineered polymerases.[17,18] TNA modifications have also been shown to enhance delivery and expression of linear DNA genes in eukaryotic cells.[19]

Our laboratory has synthesized building blocks with chirally defined methyl groups at 2′ and 5′ positions of the ribosugar and evaluated their contributions to biophysical and therapeutic behaviors of resulting siRNAs.[20,21] Intrigued by the effect of such a small group in altering biological properties as a function of chirality, we wanted to study the role of chiral C4′-methyl substitution in TNA (Figure 1). Here, we describe the synthesis of chiral C4′-methyl-substituted TNA (4′-Me-TNA) building blocks and their incorporation into oligonucleotides. The 4′-(*R*)- and the 4′-(*S*)-methyl monomers of adenine (A), guanine (G), 5-methylcytosine (^{Me}C), thymine (T), and uracil (U) were prepared as phosphoramidites and as triphosphates. Terminal

https://doi.org/10.1021/jacs.6c07051
J. Am. Chem. Soc. 2026, 148, 38692−38706

Downloaded from pubs.acs.org/jacsat/article-pdf/148/36/38692/6822318/jacs.6c07051.pdf by VANDERBILT UNIV user on 10 October 2026

Scheme 2. Synthesis of 4′-(*R*)-Me-TNA Sugar Intermediate and Syntheses of 4′-(*R*)-Me-TNA U, T, A, and G Building Blocks[a]



[a]Reagents and conditions: (i) TBDPSCl, imidazole, DMF, 80 °C, overnight; (ii) aqueous TFA (80%), DCM, room temperature, overnight, 58% in two steps; (iii) Bz_2O, DMAP, pyridine, room temperature, overnight; (iv) (a) BSA, CH_3CN, 60 °C, 30 min and (b) TMSOTf, CH_3CN, 60 °C, 2 h for U and T (**18a**,**b**); (v) (a) BSA, toluene, 90−95 °C, 30 min and (b) TMSOTf, toluene, 90−95 °C, 2 h for N^6-Bz-A (**18c**); (vi) conditions mentioned as (v) followed by TFA, DCM, 0 °C, 2 h for N^2-ibu-G (**18d**); (vii) TBAF (1.0 M in THF), THF, 0 °C, 2 h; (viii) DMT-Cl, $AgNO_3$, THF-pyridine (4:1), room temperature, overnight; (ix) aq. NaOH (1.0 M), THF-MeOH (1:1), room temperature, 3−5 h; (x) 2-cyanoethyl-*N*,*N*-diisopropylchlorophosphoramidite, NMI, DIPEA, DCM, room temperature, 30 min; (xi) (a) succinic anhydride, DMAP, DCM, room temperature, overnight, (b) LCAA-CPG, DIPEA, HBTU, DMF, mechanical shaker, overnight, and (c) Ac_2O, pyridine, mechanical shaker, room temperature, 3 h.

modification of deoxyoligonucleotides with either 4′-(*R*)- or 4′-(*S*)-Me-TNA was more resistant to nuclease degradation than were controls with a terminal deoxy residue with a phosphorothioate linkage. Thermal stability studies indicate that the 4′-(*R*) stereoisomer is more destabilizing than the 4′-(*S*) stereoisomer in the contexts of RNA and of DNA duplexes. Crystal structures of RNA duplexes that contain either 4′-(*R*)- or 4′-(*S*)-Me-TNA revealed that the 4′-(*R*) isomer causes greater distortion of the duplex than does the (*S*) isomer. Polymerase recognition studies reveal that 4′-(*R*)- and 4′-(*S*)-Me-TNA nucleotide triphosphates (NTPs) are poor substrates for polymerases that have been engineered to synthesize standard TNA oligonucleotides.

RESULTS AND DISCUSSION

Syntheses of 4′-Me-TNA Building Blocks

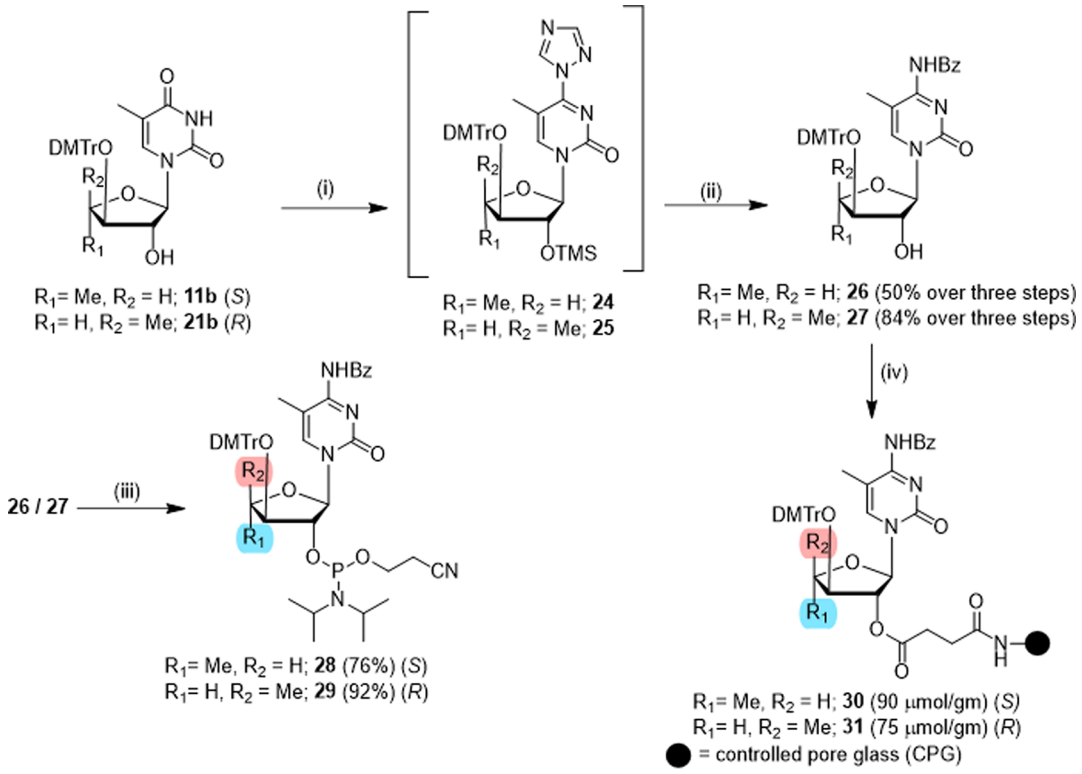
We introduced chiral methyl groups at the C4′ position of TNA as shown in Scheme 1. We first glycosylated the appropriate threose sugar intermediates. For the (*S*) isomers, we started from the previously reported sugar intermediate **1**.[22] The compound was desilylated, and the primary hydroxyl group was selectively iodinated to afford **3**. Protection of the secondary hydroxyl group and dehalogenation produced the intermediate **5**. Removal of the acetonide protecting group followed by benzoylation yielded intermediate **7** as the fully protected glycosyl donor. Scale-up of the synthesis of compound **7** provided the material needed to make the 4′-(*S*) isomers for each of the 4′-Me-TNA building blocks.

Glycosidic bond formation at the C1′ position of the 4′-modified tetrose sugar following Vorbrüggen glycosylation with uracil, thymine, N^6-benzoyladenine, or O^6-diphenylcarbamoyl-N^2-isobutyrylguanine afforded nucleoside intermediates **8a**−**d**, respectively. Removal of TBDPS groups of compounds **8a** and **8b**, followed by DMT protection of the secondary 3′-OH group, afforded uridine and thymidine analogs **10a** and **10b**, respectively. Benzoyl group deprotection of **10a** and **10b** under basic conditions produced compounds **11a** and **11b**,

https://doi.org/10.1021/jacs.6c07051
J. Am. Chem. Soc. 2026, 148, 38692−38706

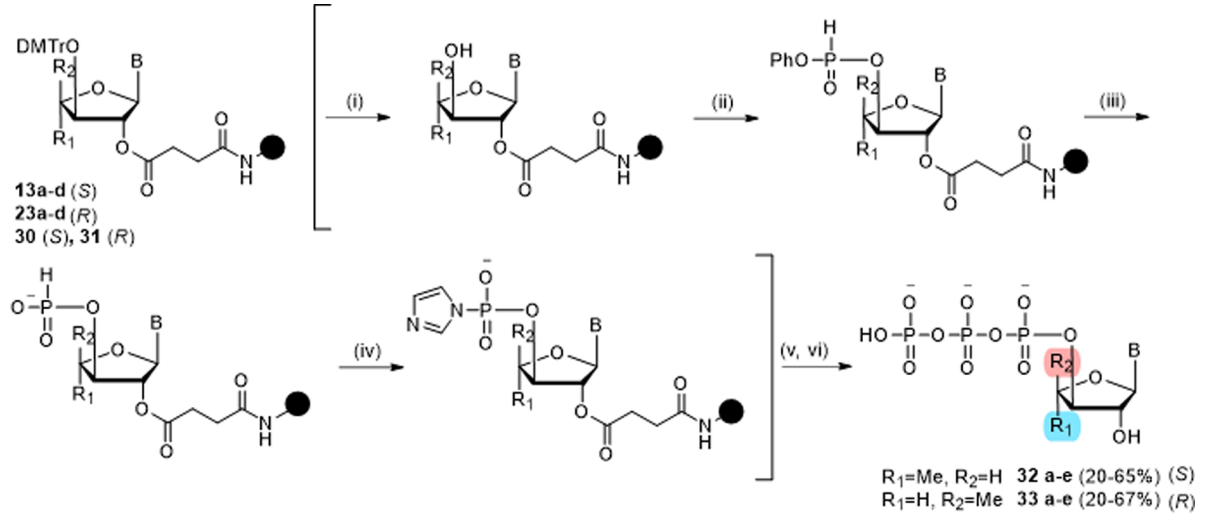
Downloaded from pubs.acs.org/jacsat/article-pdf/148/36/38692/6822318/jacs.6c07051.pdf by VANDERBILT UNIV user on 10 October 2026

Scheme 3. Syntheses of 4′-(*S*)- and 4′-(*R*)-Me-TNA C Building Blocks[a]



[a]Reagents and conditions: (i) (a) TMSCl, NEt_3, room temperature, 4 h and (b) $POCl_3$, NEt_3, 1,2,4-triazole, CH_3CN, 0 °C, 4 h; (ii) (a) NH_4OH, 1,4-dioxane, room temperature, overnight and (b) Bz_2O, DMF, room temperature, overnight; (iii) 2-cyanoethyl-*N*,*N*-diisopropylchlorophosphoramidite, NMI, DIPEA, DCM, room temperature, 30 min; (iv) (a) succinic anhydride, DMAP, DCM, room temperature, overnight, (b) LCAA-CPG, DIPEA, HBTU, DMF, mechanical shaker, overnight, and (c) Ac_2O, pyridine, mechanical shaker, room temperature, 3 h.

Scheme 4. Solid-Phase Syntheses of Chiral 4′-Me-TNA NTPs[a]



[a]Reagents and conditions: (i) trichloroacetic acid, DCM; (ii) diphenyl phosphite, anhydrous pyridine; (iii) triethylammonium bicarbonate, water, CH_3CN; (iv) BSA/$CBrCl_3$/imidazole, anhydrous CH_3CN; (v) tributylammonium pyrophosphate, anhydrous DMF; (vi) AMA, 2 or 5 h for pyrimidines and purines, respectively.

which were used to make phosphoramidites **12a** and **12b** as well as the controlled pore glass (CPG) supports **13a** and **13b**. For the adenosine derivatives, compound **8c** was desilylated, and the secondary OH group was DMT-protected to afford **10c**. Selective benzoyl deprotection of the 2′-OH group was achieved by treating **10c** under basic conditions at 0 °C for 3 h. Compound **11c** was then used to synthesize phosphoramidite **12c** and the corresponding CPG **13c** under standard conditions.[12] To prepare the guanosine analog, Vorbrüggen glycosylation was performed, and the fully protected nucleoside was treated under acidic conditions to remove the diphenyl carbamoyl (DPC) group to obtain **8d**. Desilylation of **8d**

https://doi.org/10.1021/jacs.6c07051
J. Am. Chem. Soc. 2026, 148, 38692−38706

Downloaded from pubs.acs.org/jacsat/article-pdf/148/36/38692/6822318/jacs.6c07051.pdf by VANDERBILT UNIV user on 10 October 2026

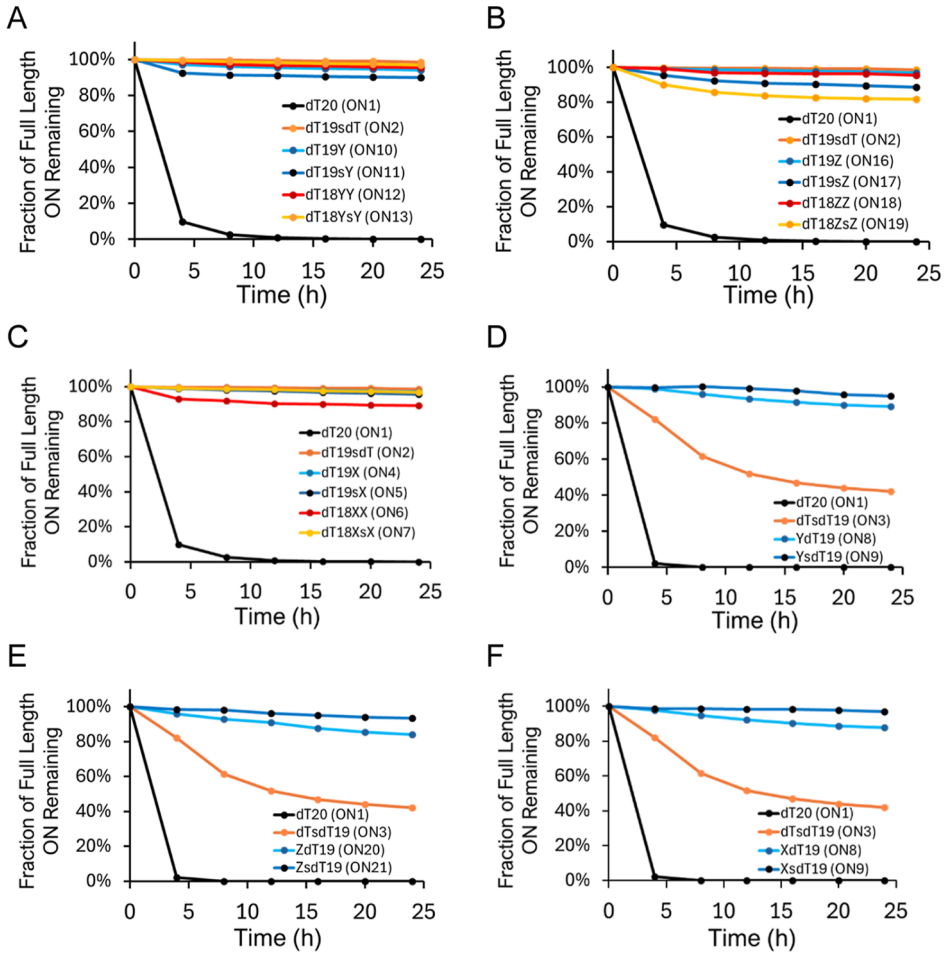


Figure 2. Terminal 4′-Me-TNA stabilizes an oligonucleotide in the presence of exonuclease to an extent comparable to a terminal TNA. Percent full-length oligonucleotides with 3′ terminal (A) 4′-(*R*)-Me-TNA-T (Y), (B) 4′-(*S*)-Me-TNA-T (Z), and (C) TNA-T (X) over time in the presence of snake venom phosphodiesterase. Percent full-length oligonucleotides with 5′ terminal (D) 4′-(*R*)-Me-TNA-T (Y), (E) 4′-(*S*)-Me-TNA-T (Z), and (F) TNA-T (X) over time in the presence of phosphodiesterase II. Here, 's' indicates phosphorothioate linkage; all other linkages were phosphodiester.

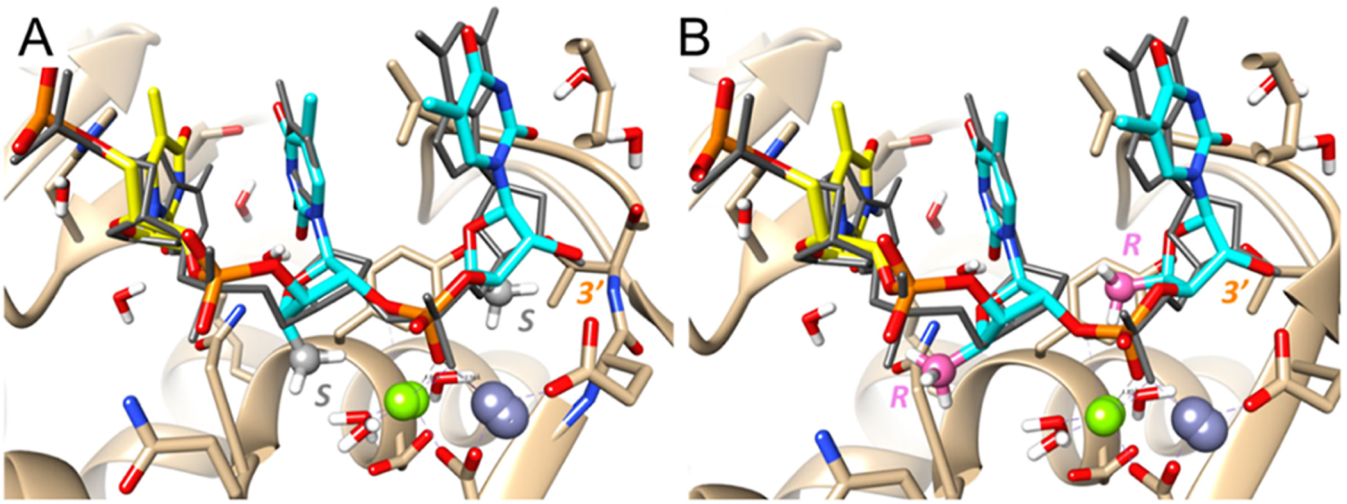


Figure 3. Models of the Klenow fragment 3′-exonuclease active site containing a substrate with a 3′-terminal (A) 4′-(*S*)-Me-TNA T and (B) 4′-(*R*)-Me-TNA T. Carbon atoms of 4′-Me-TNA residues and dT are colored in cyan and yellow, respectively, and 4′-methyl groups are depicted in vdW mode with the methyl carbon colored in gray for the (*S*) isomer and in pink for the (*R*) isomer. Phosphorus and oxygen atoms of the phosphates in the modified trimer are colored in orange and red, respectively, and Mg^{2+} and Zn^{2+} are shown as green and purple spheres, respectively, with coordinated water molecules. The 5′-d(*GCTTACG*)-3′ substrate in the PDB ID 1KFS exonuclease complex is shown with thin gray bonds; the italicized nucleotides were not visible in the crystal structure.

Downloaded from pubs.acs.org/jacsat/article-pdf/148/36/38692/6822318/jacs.6c07051.pdf by VANDERBILT UNIV user on 10 October 2026

https://doi.org/10.1021/jacs.6c07051
J. Am. Chem. Soc. 2026, 148, 38692−38706

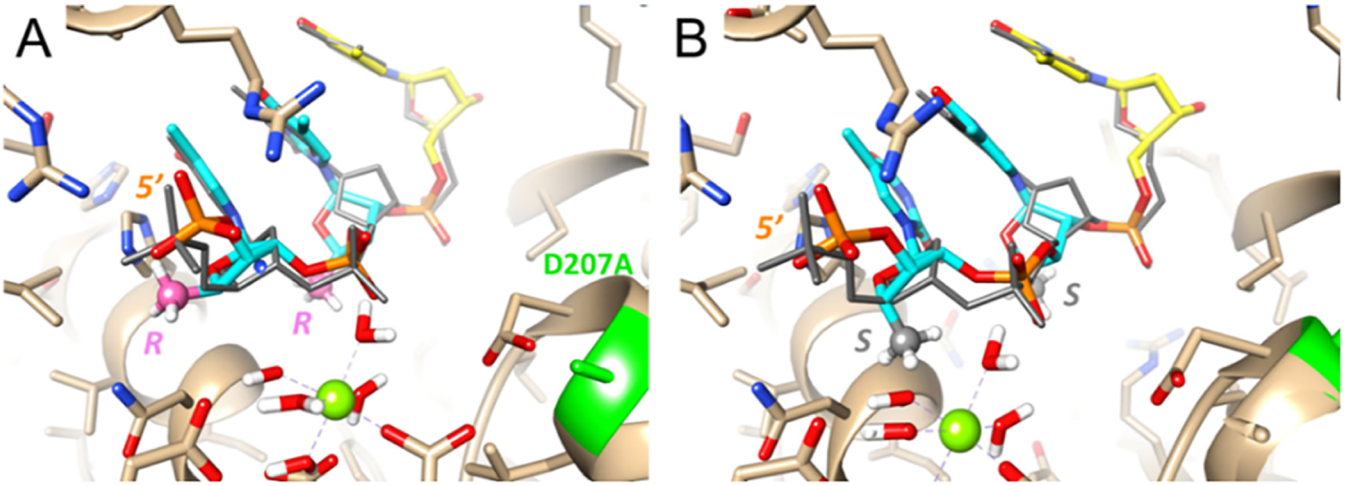


Figure 4. Models of the Xrn1 5′-exonuclease active site containing a substrate with a 5′ terminal (A) 4′-(*R*)-Me-TNA T and (B) 4′-(*S*)-Me-TNA T. Carbon atoms of the 4′-Me-TNA residues and dT are colored in cyan and yellow, respectively, and 4′-methyl groups are depicted in vdW mode with the methyl carbon colored in pink for the (*R*) isomer and in gray for the (*S*) isomer. Phosphorus and oxygen atoms of the 5′ phosphate of the modified trimer are colored in orange and red, respectively, and Mg^{2+} is shown as a green sphere with coordinated water molecules. The 5′-P-d(TTT) substrate in the parent Xrn1 complex (PDB ID 2Y35) is overlaid with thin gray bonds. Only one Mg^{2+} ion was detected in the crystal structure. Residue D207A, which was mutated in the crystallized protein to render it catalytically inactive, is indicated in green.

Table 1. Thermal Stabilities of RNA Duplexes Containing a Single 4′-(*R*)-Me-TNA[a,b,c,d]

Entry	ID	Sequences [a]	T_m (°C)[b]	ΔT_m (°C)[c]	ΔT_m with single TNA (°C) [d]
D1	**ON22**	5′-r(UACAGUCUAUGU)-3′	52.0	NA	NA
	ON23	3′-r(AUGUCAGAUACA)-5′			
D2	**ON23**	5′-r(ACAUAGACUGUA)-3′	45.5	-6.5	-2.3
	ON24	3′-r(UGUAUC**T**GACAU)-5′			
D3	**ON23**	5′-r(ACAUAGACUGUA)-3′	40.0	-12.0	-7.1
	ON26	3′-r(UGUAU**C**UGACAU)-5′			
D4	**ON22**	5′-r(UACAGUCUAUGU)-3′	43.5	-8.5	-4.6
	ON28	3′-r(AUGUC**A**GAUACA)-5′			
D5	**ON22**	5′-r(UACAGUCUAUGU)-3′	43.3	-8.7	-4.4
	ON30	3′-r(AUGUCA**G**AUACA)-5′			
D6	**ON24**	5′-r(UACAG**T**CUAUGU)-3′	33.7	-18.3	-9.4
	ON28	3′-r(AUGUC**A**GAUACA)-5′			
D7	**ON26**	5′-r(UACAGU**C**UAUGU)-3′	28.3	-23.7	-13.3
	ON30	3′-r(AUGUCA**G**AUACA)-5′			

[a]The 4′-(*R*)-Me-TNA residues are highlighted in red. [b]T_m values obtained from the maxima of the first derivatives of the (average of two heating and two cooling) melting curves (A_{260} vs temperature) recorded in PBS buffer (pH 7.4) using 2.0 μM concentrations of each strand. [c]ΔT_m is the difference in melting temperature between the test duplex and the reference RNA duplex **D1**. [d]ΔT_m is the difference in melting temperature between the test duplex and the reference duplex containing a single TNA; the T_m values were 47.8 °C for TNA T-containing duplex, 47.1 °C for TNA C-containing duplex, 48.1 °C for TNA A-containing duplex, 47.7 °C for TNA G-containing duplex, 43.1 °C for TNA A-T pair containing duplex, and 41.6 °C for TNA G-C pair containing duplex.

followed by protection of the free secondary hydroxyl group with DMT yielded **10d**. Deprotection of the benzoyl group from the 2′-OH yielded **11d**, which was then converted into the corresponding guanosine building blocks **12d** and **13d** as described for the other 4′-(*S*)-Me-TNA analogs (Scheme 1).

The 4′-(*R*)-methoxymethyl-TNA was previously synthesized by the Fernandes group from D-xylose.[23] Recently, an epimer of

https://doi.org/10.1021/jacs.6c07051
J. Am. Chem. Soc. 2026, 148, 38692−38706

Downloaded from pubs.acs.org/jacsat/article-pdf/148/36/38692/6822318/jacs.6c07051.pdf by VANDERBILT UNIV user on 10 October 2026

Table 2. Thermal Stabilities of RNA Duplexes Containing a Single 4′-(*S*)-Me-TNA[a,b,c,d]

Entry	ID	Sequences [a]	T_m (°C) [b]	ΔT_m (°C)[c]	ΔT_m with single TNA (°C)[d]
D1	**ON22**	5′-r(UACAGUCUAUGU)-3′	52.0	NA	NA
	ON23	3′-r(AUGUCAGAUACA)-5′			
D8	**ON23**	5′-r(ACAUAGACUGUA)-3′	49.0	-3.0	+1.2
	ON25	3′-r(UGUAUCTGACAU)-5′			
D9	**ON23**	5′-r(ACAUAGACUGUA)-3′	45.2	-6.8	-1.9
	ON27	3′-r(UGUAUCUGACAU)-5′			
D10	**ON22**	5′-r(UACAGUCUAUGU)-3′	46.0	-6.0	-2.1
	ON29	3′-r(AUGUCAGAUACA)-5′			
D11	**ON22**	5′-r(UACAGUCUAUGU)-3′	46.2	-5.8	-1.5
	ON31	3′-r(AUGUCAGAUACA)-5′			
D12	**ON25**	5′-r(UACAGTCUAUGU)-3′	40.3	-11.7	-2.8
	ON29	3′-r(AUGUCAGAUACA)-5′			
D13	**ON27**	5′-r(UACAGUCUAUGU)-3′	38.8	-13.2	-2.8
	ON31	3′-r(AUGUCAGAUACA)-5′			

[a]The 4′-(*S*)-Me-TNA residues are highlighted in cyan. [b]T_m values obtained from the maxima of the first derivatives of the (average of two heating and two cooling) melting curves (A_{260} vs temperature) recorded in PBS buffer (pH 7.4) using 2.0 μM concentrations of each strand. [c]ΔT_m is the difference in melting temperature between the test duplex and the reference RNA duplex **D1**. [d]ΔT_m is the difference in melting temperature between the test duplex and the reference duplex containing a single TNA; the T_m values were 47.8 °C for TNA T-containing duplex, 47.1 °C for TNA C-containing duplex, 48.1 °C for TNA A-containing duplex, 47.7 °C for TNA G-containing duplex, 43.1 °C for TNA A-T pair containing duplex, and 41.6 °C for TNA G-C pair containing duplex.

TNA that combines structural features from inverted-dT and TNA has been reported.[24] We synthesized 4′-(*R*)-Me-TNA building blocks as shown in Scheme 2. We began by protecting the secondary OH group of intermediate **14**, prepared as reported previously,[25] with TBDPS to afford **15**. The acetonide group was then removed under acidic conditions to obtain **16**, which was benzoylated to afford the key intermediate **17** (Scheme 2). The sugar intermediate **17** was then used to synthesize (*R*) isomers of 4′-Me-TNA building blocks as phosphoramidites (**22a−d**) and as CPGs (**23a−d**) using synthetic routes described for syntheses of the (*S*) isomers.

The 4′-Me-TNA cytidine analogs were synthesized from the DMT-protected pyrimidine precursor (Scheme 3). The (*S*) and (*R*) isomers of thymidine building block, **11b** and **21b**, respectively, were C4-triazolylated with concomitant TMS protection of the 2′-OH group. Intermediates **24** and **25** were treated with aqueous ammonia without further purification to afford the 3′-DMT-protected analogs. The C4-amino groups of these intermediates were selectively benzoylated to obtain the (*S*) and (*R*) isomers **26** and **27**, respectively. Compound **26** was used to make the phosphoramidite **28** and CPG **30** building blocks. Similarly, the building blocks for the (*R*) isomer obtained from **27** were converted into phosphoramidite **29** and CPG **31**.

Oligonucleotide Synthesis

A series of oligonucleotides with terminal 4′-(*R*)- and (*S*)-Me-TNA analogs were synthesized to assess exonuclease resistance (Table S1). We also synthesized oligonucleotides containing internal 4′-Me-TNA modifications for thermal melting analysis and crystal structure studies (Tables S2 and S3). We also synthesized sense and antisense strands of the sequences of those of a previously described siRNA targeting mouse *Ttr* that were fully modified with either 4′-(*R*)- or 4′-(*S*)-Me-TNA (Table S4) to demonstrate the synthetic feasibility of fully modified Me-TNA oligonucleotides. For deprotection of *N*4-benzoyl-5-methylcytosine in oligonucleotides, either 28−30% ammonium hydroxide solution containing 5% DEA at 60 °C for 5 h or 40% aq. methylamine ($MeNH_2$) solution at 65 °C for 12 min was used, and complete deprotection of benzoyl group was observed for these Me-TNA monomers in both conditions. This was confirmed by the MS data, which were consistent for the above deprotection protocols. All conditions related to phosphoramidite coupling, deprotection from solid support and purification are fully described in the Supporting Information.

Syntheses of 4′-Me-TNA NTPs

We used a previously described *H*-phosphonate chemistry protocol[26] to synthesize triphosphates of the chiral TNA analogs (**32a−e** and **33a−e** for (*S*)- and (*R*)-analogs, respectively) in 10 μmol scale in five steps: detritylation, phosphitylation, hydrolysis, oxidation, and nucleophilic substitution (Scheme 4). First, compounds **13a−d**, **23a−d**, **30**, and **31** were detritylated with 3% trichloroacetic acid in DCM.[27] Subsequent steps were automated following our previously established protocol.[26] Briefly, the 3′-alcohols were phosphitylated using diphenyl phosphite to obtain *H*-phosphonate monoesters. Subsequent hydrolysis with aqueous triethylammonium bicarbonate yielded corresponding 3′-*H*-phosphonates that were oxidized with *N*,*O*-bis(trimethylsilyl)acetamide (BSA), bromotrichloromethane, and imidazole to yield 3′-phosphorimidazolidates. Finally, nucleophilic attack by the pyrophosphate anion

Downloaded from pubs.acs.org/jacsat/article-pdf/148/36/38692/6822318/jacs.6c07051.pdf by VANDERBILT UNIV user on 10 October 2026

https://doi.org/10.1021/jacs.6c07051
J. Am. Chem. Soc. 2026, 148, 38692−38706

Table 3. Thermal Stabilities of RNA Duplexes Containing 4′-Me-TNA Pairs of the Same and Different Chiralities[a,b,c,d,e,f]

Entry	ID	Sequences [a]	T_m (°C) [b]	ΔT_m vs. RNA/RNA (°C) [c]	ΔT_m vs. duplex with TNA pair (°C) [d]	ΔT_m vs. duplex with (*R*) isomer pair (°C) [e]	ΔT_m vs. duplex with (*S*) isomer pair (°C) [f]
D1	**ON22**	5′-r(UACAGTCUAUGU)-3′	52.0	NA	NA	NA	NA
	ON23	3′-r(AUGUCAGAUACA)-5′					
D14	**ON42**	5′-r(UACAGTCUAUGU)-3′	43.1	-8.9	NA	+9.4	+2.8
	ON44	3′-r(AUGUCAGAUACA)-5′					
D15	**ON42**	5′-r(UACAGTCUAUGU)-3′	37.0	-15.0	-6.1	+3.3	-3.3
	ON28	3′-r(AUGUCAGAUACA)-5′					
D16	**ON42**	5′-r(UACAGTCUAUGU)-3′	40.6	-11.4	-2.5	+6.9	+0.3
	ON29	3′-r(AUGUCAGAUACA)-5′					
D6	**ON24**	5′-r(UACAGTCUAUGU)-3′	33.7	-18.3	-9.4	NA	-6.6
	ON28	3′-r(AUGUCAGAUACA)-5′					
D12	**ON25**	5′-r(UACAGTCUAUGU)-3′	40.3	-11.7	-2.8	+6.6	NA
	ON29	3′-r(AUGUCAGAUACA)-5′					
D17	**ON24**	5′-r(UACAGTCUAUGU)-3′	36.0	-16.0	-7.1	+2.3	-4.3
	ON29	3′-r(AUGUCAGAUACA)-5′					
D18	**ON25**	5′-r(UACAGTCUAUGU)-3′	35.6	-16.4	-7.5	+1.9	-4.7
	ON28	3′-r(AUGUCAGAUACA)-5′					
D19	**ON43**	5′-r(UACAGTCUAUGU)-3′	41.6	-10.4	NA	+13.3	+2.8
	ON45	3′-r(AUGUCAGAUACA)-5′					
D7	**ON26**	5′-r(UACAGTCUAUGU)-3′	28.3	-23.7	-13.3	NA	-10.5
	ON30	3′-r(AUGUCAGAUACA)-5′					
D13	**ON27**	5′-r(UACAGTCUAUGU)-3′	38.8	-13.2	-2.8	+10.5	NA
	ON31	3′-r(AUGUCAGAUACA)-5′					
D20	**ON26**	5′-r(UACAGTCUAUGU)-3′	32.6	-19.4	-9.0	+4.3	-6.2
	ON31	3′-r(AUGUCAGAUACA)-5′					
D21	**ON27**	5′-r(UACAGUCUAUGU)-3′	34.8	-17.2	-6.8	+6.5	-4.0
	ON30	3′-r(AUGUCAGAUACA)-5′					

[a]The 4′-(*R*)-Me-TNA, 4′-(*S*)-Me-TNA, and TNA are highlighted in red, cyan, and dark blue, respectively. [b]T_m values obtained from the maxima of the first derivatives of the (average of two heating and two cooling) melting curves (A_{260} vs temperature) recorded in PBS buffer (pH 7.4) using 2.0 μM concentrations of each strand. [c]ΔT_m is the difference in melting temperature between the test duplex and the reference RNA duplex **D1**. [d]ΔT_m is the difference in melting temperature between the test duplex and the reference duplex containing a TNA pair; the T_m values were 43.1 °C for the TNA A-T-containing duplex and 41.6 °C for the TNA G-C-containing duplex. [e]ΔT_m is the difference in melting temperature between the test duplex and the reference duplex containing 4′-(*R*)-Me-TNA A-T pair or the reference duplex containing the 4′-(*R*)-Me-TNA G-C pair. [f]ΔT_m is the difference in melting temperature between the test duplex and the reference duplex containing 4′-(*S*)-Me-TNA A-T pair or the reference duplex containing the 4′-(*S*)-Me-TNA G-C pair.

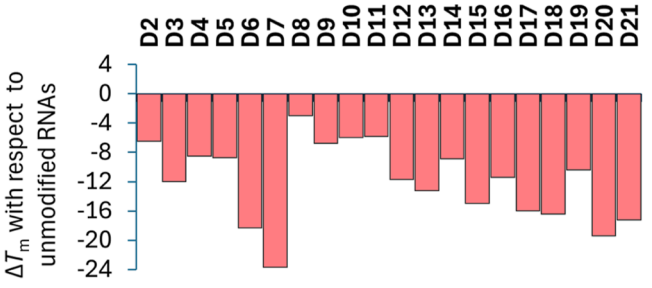


Figure 5. ΔT_m values for 4′-(*R*)- and 4′-(*S*)-Me-TNA-modified duplexes relative to unmodified RNA in the case of single incorporation and base-paired with regular TNA or chiral 4′-Me-TNAs.

on the 3′-phosphorimidazolidates generated desired 3′-triphosphates. The products were released from the solid support by treating with ammonia/methylamine solution (1:1) (AMA) for 2 h for pyrimidines and 5 h for purine monomers. The NTPs were purified by anion-exchange HPLC using 0−100% TEAB in water. The products were lyophilized, resuspended in water, and then passed through sodium ion-exchange resin to obtain desired 4′-Me-TNA NTPs as sodium salts in 20−65% yields (Table S5).

Terminal 4′-Me-TNA Residues Protect Oligonucleotides from Exonuclease-Mediated Degradation

To assess the impact of a chiral 4′-Me-TNA modification on exonuclease-mediated degradation of oligonucleotides, 4′-(*R*)- and 4′-(*S*)-Me-TNA T residues were incorporated at either the 3′ or 5′ end of a poly(T) oligodeoxynucleotide. The chiral TNA building blocks were linked through a phosphodiester linkage or a phosphorothioate linkage. The oligonucleotides were treated with 3′- or 5′-specific exonuclease, and the amount of full-length oligonucleotide was quantified over time by ion-exchange HPLC. The oligonucleotides with a single (*R*) isomer at the

Downloaded from pubs.acs.org/jacsat/article-pdf/148/36/38692/6822318/jacs.6c07051.pdf by VANDERBILT UNIV user on 10 October 2026

https://doi.org/10.1021/jacs.6c07051
J. Am. Chem. Soc. 2026, 148, 38692−38706

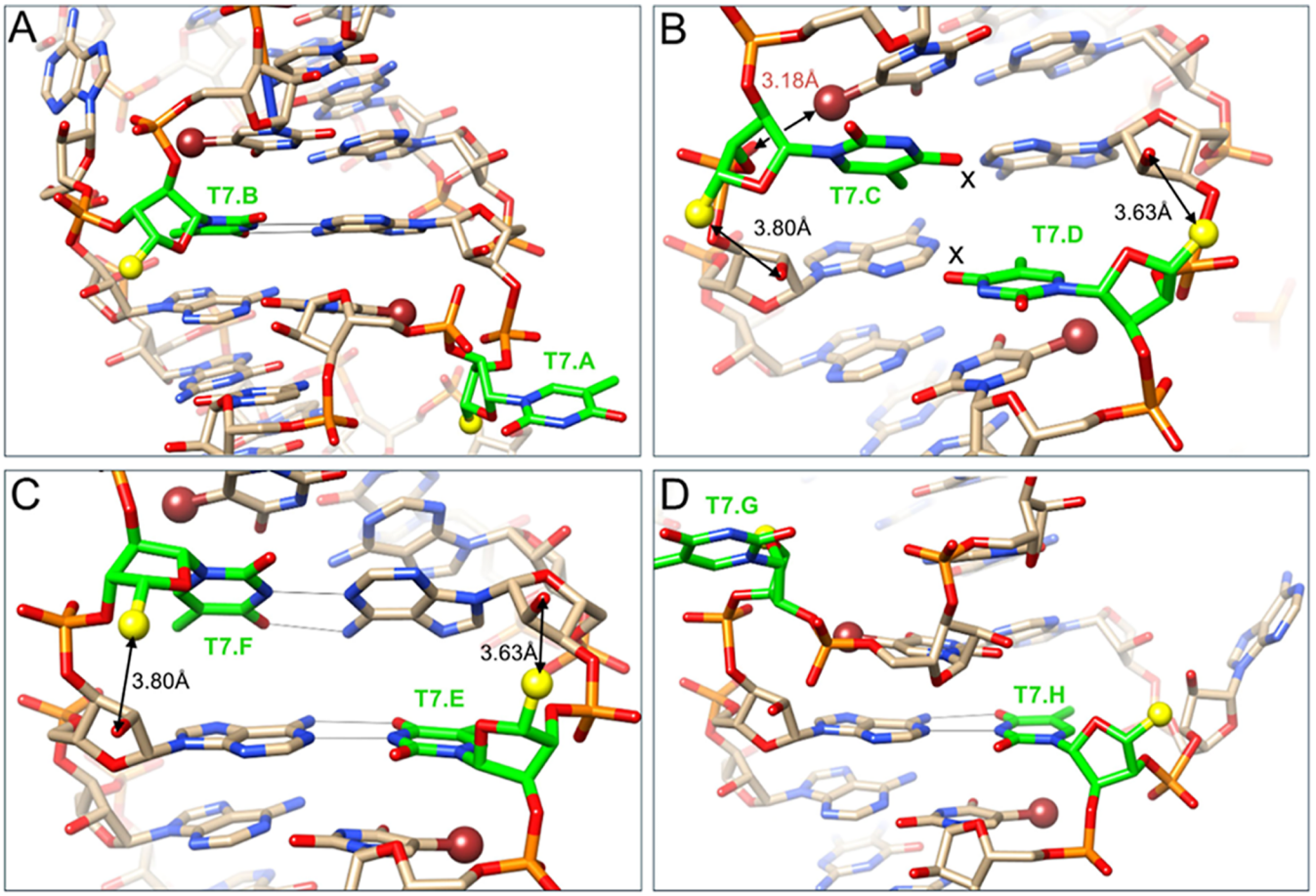


Figure 6. Pairing properties of 4′-(*R*)-Me-TNA T residues in duplexes (A) A:B, (B) C:D, (C) E:F, and (D) G:H in the asymmetric unit of the 12-mer crystal structure. Carbon atoms of 4′-(*R*)-Me-TNA Ts are colored in green, and the 4′-methyl carbon and ^{5Br}**U** bromine atoms are highlighted as spheres colored in yellow and maroon, respectively. Arrows are labeled with distances of halogen bonds, and contacts between 4′-methyl carbons and 2′-hydroxyl oxygens shorter than 4 Å. Selected hydrogen bonds are shown as thin solid lines. The "***x***" in panel B indicates the absence of Watson−Crick hydrogen bonds between 4′-(*R*)-Me-TNA T and A.

3′ termini were slightly more stable than those with an (*S*) isomer in the presence of the 3′-exonuclease snake venom phosphodiesterase whether the terminal linkage was phosphodiester or a phosphorothioate; both were considerably more stable than the deoxyoligonucleotide controls (Figure 2A,B). The TNA modification linked through phosphodiester or phosphorothioate had a resistance profile similar to that of the (*R*) isomer of the 4′-Me-TNA (Figure 2C). Incorporation of two 4′-Me-TNAs of either isomer at the 3′ termini resulted in stabilities similar to that of the oligonucleotide with a single 4′-(*R*)-Me-TNA (Figure 2A,B). At the 5′ terminus, both isomers of 4′-Me-TNA protected oligonucleotides from degradation by the 5′-exonuclease phosphodiesterase II to an extent similar to TNA irrespective of whether the terminal linkage was phosphodiester or phosphorothioate (Figure 2D−F). In summary, oligonucleotides with terminal 4′-Me-TNA or terminal TNA residues had considerably longer half-lives than the deoxyoligonucleotide controls.

Next, we used computational modeling of 4′-(*R*)- and 4′-(*S*)-Me-TNA-modified DNAs lodged at the active sites of exonucleases to obtain a qualitative understanding of how these modifications protect an oligonucleotide from exonuclease-mediated degradation. The interactions at the active site of a 3′-exonuclease were modeled based on the crystal structure of *Escherichia coli* DNA polymerase I Klenow exonuclease in complex with a short DNA fragment (PDB ID 1KFS).[28] To visualize potentially unfavorable interactions of 4′-methyl groups at the active site of a 5′-exonuclease, we used the crystal structure of *D. melanogaster* Xrn1 in complex with 5′-P-d(TTT) (PDB ID 2Y35).[29] The terminal and penultimate 2′-deoxynucleotides at either end were replaced by 4′-(*R*)- or 4′-(*S*)-Me-TNA nucleotides using the UCSF Chimera suite.[30] Subsequently, models were energy-minimized with Amber[31] (https://ambermd.org/) as implemented in UCSF Chimera using steepest descent and conjugate gradient algorithms until convergence.

The models revealed some differences in the orientations of phosphate groups depending on the chirality of the 4′-Me-TNA modification. At the Klenow fragment 3′-exonuclease active site, phosphate orientations in the 4′-(*S*)-Me-TNA-modified strand had a somewhat smaller change relative to the corresponding moieties in the DNA substrate than the phosphates in the 4′-(*R*)-Me-TNA-modified strand (Figure 3A,B). This is consistent with the slightly increased protection from nuclease degradation seen for the (*R*) relative to the (*S*) isomer (Figure 2A,B). In both cases, metal ions shifted slightly relative to the structure with DNA bound. This is noteworthy because direct interference of the *Sp*-phosphorothioate moiety with metal ion binding is thought to be the reason for the much higher stability of oligonucleotides with this isomer as the terminal linkage against

Downloaded from pubs.acs.org/jacsat/article-pdf/148/36/38692/6822318/jacs.6c07051.pdf by VANDERBILT UNIV user on 10 October 2026

https://doi.org/10.1021/jacs.6c07051
J. Am. Chem. Soc. 2026, 148, 38692−38706

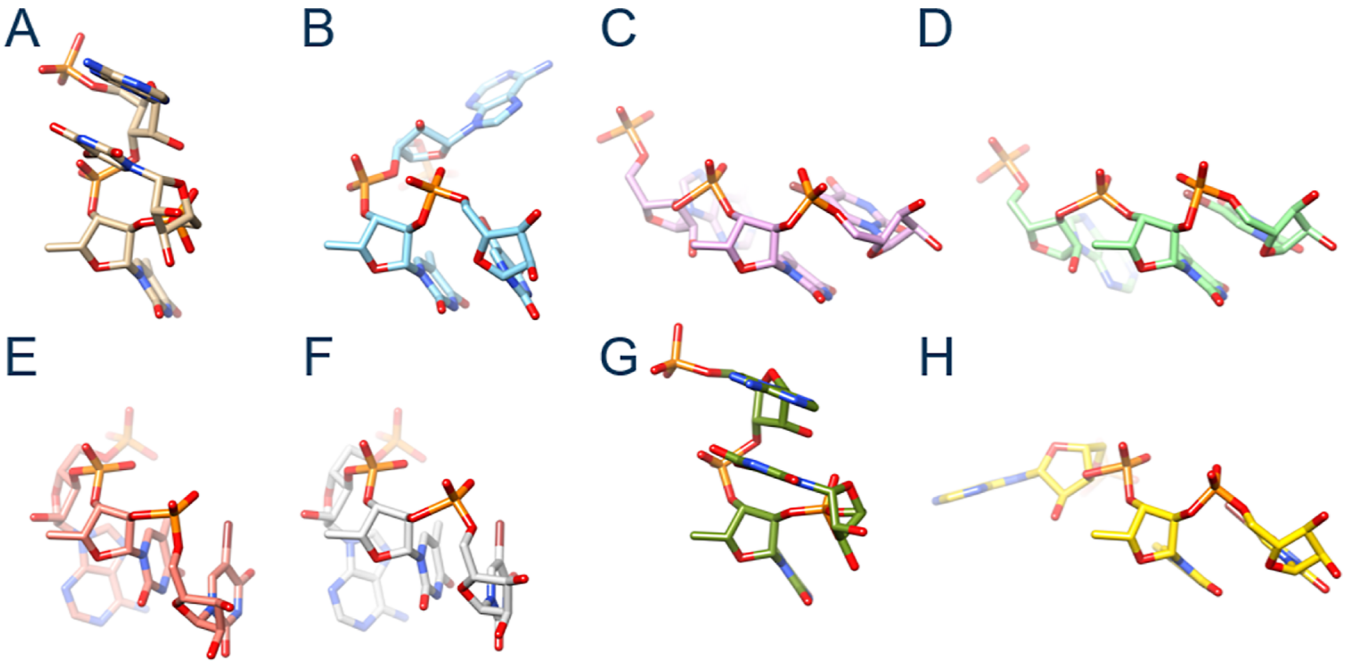


Figure 7. Comparison of the conformations of trinucleotides at positions 6, 7, and 8 in the eight strands (A-H) of the four duplexes in the asymmetric unit of the crystal structure of 5′-r(CGCGAAT^{5Br}UAGCG)-3′, where **T** is 4′-(*R*)-Me-TNA T and ^{5Br}**U** is 5-bromouridine. The views are along the normal to the best plane defined by the threose ring. All 4′-(*R*)-Me-TNAs adopt the C4′-exo pucker; no short contacts are observed for 4′-methyl substituents.

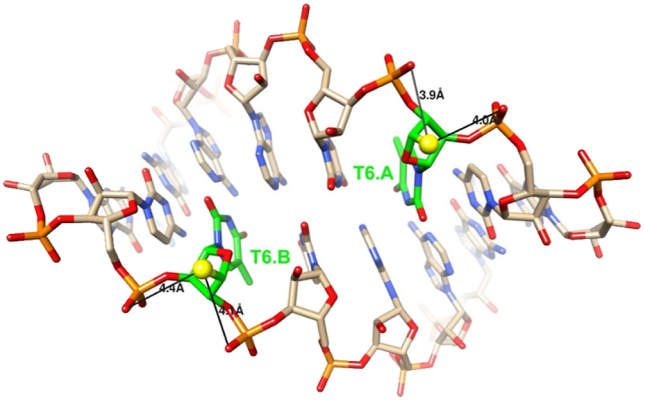


Figure 8. Crystal structure of the octamer 5′-r(^{5Br}CGAAUTCG)-3′ (**T** = 4′-(*S*)-Me-TNA T and ^{5Br}**C** is 5-bromocytidine). The duplex is viewed from the minor groove, approximately along the molecular 2-fold rotation axis. Carbon atoms of 4′-(*S*)-Me-TNA T are highlighted in green, the 4′-(*S*)-methyl carbon is shown as a yellow sphere, and selected distances to adjacent phosphate oxygens are drawn as solid lines.

3′-exonuclease degradation compared to those with a terminal *R*p stereoisomer.[28] We note, however, that TNA affords exceptionally high nuclease resistance without the additional methyl substituent (Figure 2C).

When modeled in the Xrn1 5′-exonuclease active site, the 4′-methyl group of the terminal (*R*) isomer is positioned in proximity of the 5′-phosphate group (C···P distance of 3.3 Å; Figure 4A). The methyl group of the (*S*) isomer is directed toward the Mg^{2+} ion and positioned approximately 3.2 Å from a water molecule coordinated to this metal ion (Figure 4B). Both methyl groups jut into polar environments. Despite different conformations, both isomers and the TNA backbone provide protection from digestion by 5′-exonuclease (Figure 2D−F).

4′-Me-TNA Residues Thermodynamically Destabilize RNA Duplexes

A series of 12-mer RNA oligonucleotides with single 4′-Me-TNA residues were synthesized in order to evaluate the effects of chiral TNA analogs on the thermal stabilities of antiparallel, Watson−Crick RNA duplexes. The differences in thermal melting temperatures (T_ms) between the modified duplex and the all-RNA control duplex (ΔT_m values) were calculated. A single incorporation of 4′-(*R*)-Me-TNA destabilized an otherwise all-RNA duplex by 6.5 to 12.0 °C, depending on the nucleobase, relative to the unmodified RNA control duplex (Table 1). Placement of 4′-(*R*)-Me-TNA on each strand opposite to each other in a duplex causes as much as 23.7 °C destabilization. The (*S*) isomer was less destabilizing than the (*R*) isomer: the duplexes with single incorporations of the (*S*) isomer had ΔT_m values of −3 to −6.8 °C (Table 2). Incorporation of 4′-(*S*)-Me-TNA on both strands opposite each other in a duplex causes as much as 13.2 °C destabilization. We previously reported that the incorporation of a single TNA residue reduces the stability of an RNA duplex by about 5.0 °C[12]. With the exception of the duplex **D8**, which has a single 4′-(*S*)-Me-TNA T, all other duplexes containing a chirally pure 4′-Me-TNA were less stable than those containing a single TNA (Tables 1 and 2). The thermal stabilities of oligonucleotides containing chiral 4′-Me-TNA in the RNA strand of an RNA/DNA duplex were also measured (Tables S6−S11). The 4′-Me-TNA purines were destabilizing by 7.3 to 12.8 °C, and 4′-Me-TNA pyrimidines were destabilizing by 4.7 to 9.5 °C (Tables S6 and S7). When the 4′-Me-TNA was incorporated into the DNA strand of an RNA/DNA hybrid, purines were less destabilizing than pyrimidines (Tables S8−S11).

We next evaluated the effects of a base pair formed by 4′-Me-TNA residues of different and of the same chiralities on the thermal stability of an otherwise RNA duplex. For TNA base pairs, the destabilization was additive.[12] In contrast, the net

https://doi.org/10.1021/jacs.6c07051
J. Am. Chem. Soc. 2026, 148, 38692−38706

Downloaded from pubs.acs.org/jacsat/article-pdf/148/36/38692/6822318/jacs.6c07051.pdf by VANDERBILT UNIV user on 10 October 2026

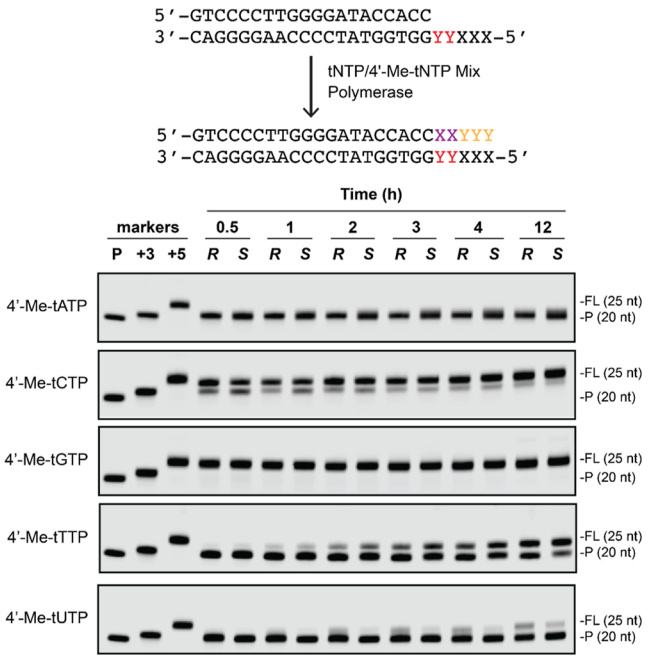


Figure 9. Chiral 4′-(*R*)- and 4′-(*S*)-Me-TNA triphosphates are poor substrates for a TNA polymerase. Upper: schematic of the polymerization reaction. Color scheme for the primer extension reaction: incoming 4′-(*R*)- or 4′-(*S*)-Me-TNA triphosphate (purple **X**), DNA base templating the addition of the 4′-(*R*)- or 4′-(*S*)-Me-TNA triphosphate (red **Y**), normal TNA additions (yellow **Y**), and the DNA base templating the addition of normal TNA triphosphates (black **X**). Lower: reaction progress over time analyzed by denaturing PAGE. Reaction progress over time was analyzed by denaturing PAGE using eight different TNA triphosphate mixtures in which each nucleotide was individually replaced with its corresponding 4′-(*R*)- or 4′-(*S*)-Me-TNA triphosphate; the identity of the 4′-Me-TNA triphosphate substitution is indicated to the left of the gel with the *R* and *S* isomer denoted above the gel lanes. Time points were taken for 0.5, 1, 2, 3, 4, and 12 h. Markers are the 20-mer primer strand (P) and oligonucleotides of 23 (+3) and 25 (+5) nucleotides. The locations of the primer (P) and the full-length 25-nucleotide product (FL) are indicated to the right of the gel.

stability of duplexes with chiral 4′-Me-TNAs varied depending on the chirality and sequence (Table 3 and Figure 5). The T_m values for duplexes with (*S*)-(*R*) or (*R*)-(*S*) chirality pairs were higher than those of the duplexes with the (*R*)-(*R*) chiralities for both A-T and G-C pairs. In contrast, the T_m values were lower for the duplexes with mixed chiralities than for duplexes with (*S*)-(*S*) A-T or (*S*)-(*S*) G-C base pairs (Table 3). Further, we observed that the 4′-Me-TNA G-C base pairs were less thermally stable than the 4′-Me-TNA A-T base pairs, as previously reported for TNA.[4,32] The base pairs between 4′-Me-TNA and TNA were less stable than were TNA−TNA base pairs but more stable than the chiral pairs.

The Crystal Structures of RNA Duplexes Containing Chirally Pure 4′-Me-TNA Residues Reveal Reasons for Different Impacts on Duplex Stability

We solved the crystal structures of a 12-mer RNA duplex, 5′-r(CGCGAAT^{5Br}UAGCG)-3′, where **T** is 4′-(*R*)-Me-TNA T, and of an 8-mer duplex, 5′-r(^{5Br}CGAAUTCG)-3′, where **T** is 4′-(*S*)-Me-TNA T. Diffraction data for the crystal of the 12-mer with space group $P2_1$ were phased with 5-bromouridine (^{5Br}**U**). The structure was determined at 1.54 Å resolution and contained four duplexes per crystallographic asymmetric unit (Figure S1 and Table S12). The eight 4′-(*R*)-Me-TNA residues in the asymmetric unit have different orientations and pairing properties. In the A:B duplex, the 4′-(*R*)-Me-TNA T of strand A is looped out of the helix, and the 4′-(*R*)-Me-TNA T in strand B forms a Watson−Crick base pair with A from the opposite strand (Figure 6A). In the C:D duplex, both 4′-(*R*)-Me-TNA T residues are stacked inside the helix but do not form hydrogen bonds with As from the opposite strand (Figure 6B). In the C strand, the bromine from ^{5Br}**U** in position 8 is halogen-bonded to OP1 from the 4′-(*R*)-Me-TNA T (3.18 Å). In the E:F duplex, both 4′-(*R*)-Me-TNA T residues form standard A:T pairs (Figure 6C). In the G:H duplex, the 4′-(*R*)-Me-TNA T of strand G is looped out of the helix and the complementary T in strand H forms a Watson−Crick base pair with an A on the opposite strand (Figure 6D). As in the case of the A:B duplex, the orphaned A adopts an extrahelical orientation.

The α-(L)-threofuranosyl moieties of each of the eight 4′-(*R*)-Me-TNA nucleotides in the asymmetric unit adopt the C4′-exo pucker, which is the preferred conformation of the unmodified threose sugar.[12] Despite identical sugar puckers, the conformations of 4′-(*R*)-Me-TNA nucleotides vary considerably as shown by the comparison of structures of the eight trinucleotides in positions 6, 7, and 8 (Figure 7 and Figure S2). In three of four duplexes in the crystal structure, the bases of the 4′-(*R*)-Me-TNA residues do not stack or form hydrogen bonds. This likely results in the decreased thermal stability of the RNA duplex containing a 4′-(*R*)-Me-TNA residue compared to those containing a TNA or 4′-(*S*)-Me-TNA residue.

The crystal structure of the octamer containing 4′-(*S*)-Me-TNA T was solved at 2.6 Å resolution using a combination of Br single-wavelength anomalous dispersion and molecular replacement. In contrast to the crystal of the duplex that contains 4′-(*R*)-Me-TNA, the crystal of the duplex containing 4′-(*S*)-Me-TNA T contains a single duplex per asymmetric unit in space group *R*3. Bases of 4′-(*S*)-Me-TNA T residues are stacked inside the duplex and engage in Watson−Crick pairing with adenosine residues (As) on the opposite strands (Figure 8). Both 4′-(*S*)-methyl tetroses adopt the C4′-exo pucker as was observed for duplexes containing TNA and 4′-(*R*)-Me-TNA. The O4′-exo pucker type was seen in molecular dynamics simulations of a TNA dodecamer duplex.[33] The lack of conformational variability and the stacked and paired conformation of 4′-(*S*)-Me-TNA Ts within the RNA duplex is consistent with the smaller loss of thermal stability compared with a duplex containing the (*R*) isomer.

Support for the hypothesis that unfavorable interactions between the methyl group of 4′-(*R*)-Me-TNA and neighboring moieties in the duplex underlie the thermal destabilization was also obtained from analysis of nearest neighbor interactions for 4′-(*R*)- and 4′-(*S*)-methyl groups added to threose sugars in the NMR solution structure of the TNA duplex [t-(CGAATTCG)]$_2$.[5] Inspection of the model revealed more serious clashes for 4′-(*R*)-methyl groups than the 4′-(*S*)-methyl group, particularly with the 3′-phosphate group (Figure S3). Conversely, the 4′-(*S*)-methyl groups do not have short contacts to the OP1 oxygen atoms of 3′- and 2′-adjacent phosphates in the octamer duplex (Figure 8).

4′-(*R*)- and 4′-(*S*)-Me-TNA 3′-Triphosphates Are Poor TNA Polymerase Substrates

We evaluated the ability of an engineered TNA polymerase to recognize the chiral 4′-(*R*)- and 4′-(*S*)-Me-TNA 3′-triphosphate substrates in a primer extension assay.[34] For this

Downloaded from pubs.acs.org/jacsat/article-pdf/148/36/38692/6822318/jacs.6c07051.pdf by VANDERBILT UNIV user on 10 October 2026

https://doi.org/10.1021/jacs.6c07051
J. Am. Chem. Soc. 2026, 148, 38692−38706

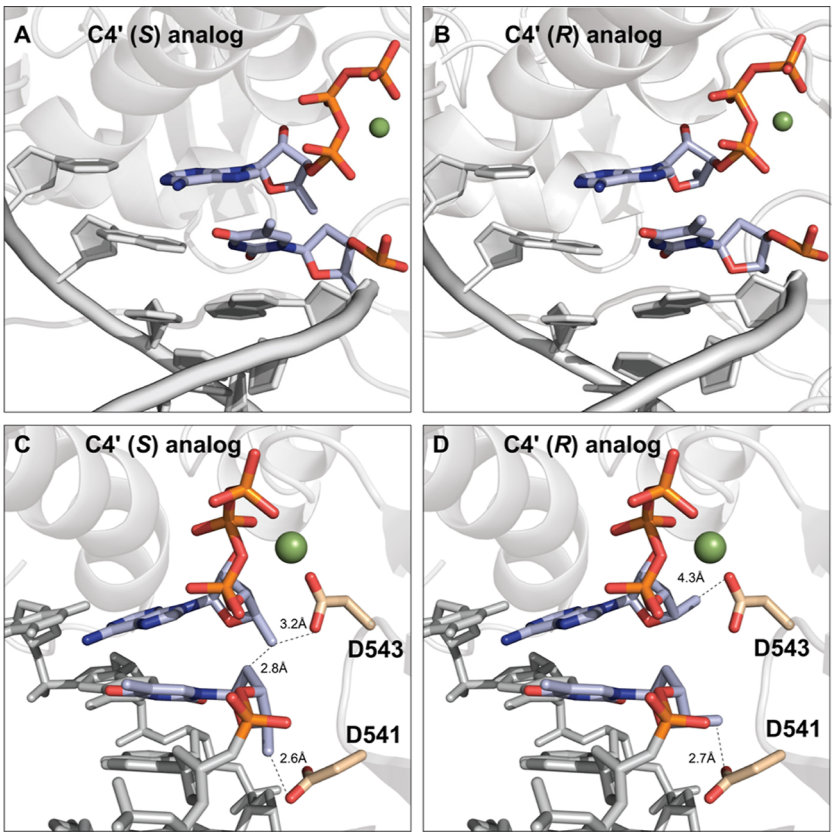


Figure 10. Chiral 4′-(*R*)- and 4′-(*S*)-Me-TNA triphosphates are poorly accommodated in the active site of the polymerase. The PDB ID for the closed ternary structure of the evolved 10−92 TNA polymerase (TNAP) is **8T3X** with 4′-(*R*)- and 4′-(*S*)-Me-TNA residues modeled in place of the 2′-deoxy-TNA residues used to capture the polymerase in a closed conformation. (A,B) View of the Watson−Crick base pair formed between the DNA template and (A) 4′-(*S*)- or (B) 4′-(*R*)-Me-TNA. (C,D) View of close contacts with nearby catalytic aspartate residues and primer (*S* isomer only). The protein and DNA portions of the template are shown in gray. The Mg^{2+} ion is shown as the green ball. Me group position and chirality are shown in each panel. TNA residues are colored by atom: carbon (purple), nitrogen (blue), oxygen (red), and phosphorus (orange). Aspartate side chains are colored by atom: carbon (wheat) and oxygen (red).

experiment, we chose 10−92, a TNA polymerase that was selected using directed evolution to synthesize TNA with a rate of ∼1 nucleotide/second with >99.9% fidelity.[35] For the primer extension assay, a DNA primer was annealed to a DNA template resulting in a 5-nucleotide unpaired region in the template strand. The 10−92 polymerase was challenged to extend the primer using a TNA triphosphate mixture in which each nucleotide was individually replaced with its corresponding 4′-(*R*)- or 4′-(*S*)-Me-TNA triphosphate. The 4′-(*R*)- and 4′-(*S*)-Me-TNA triphosphates for tA, tT, and tU were strong inhibitors of primer extension, as evidenced by the high level of chain termination observed even under prolonged incubation times of up to 12 h (Figure 9). Read through was observed for 4′-(*R*)- or 4′-(*S*)-Me-TNA triphosphates of tG and tC; however, subtle shifts in band mobility imply that the elongated product likely contains one or more misincorporation events due to TNA mispairing opposite either dC or dG in the template. Such a result is not unexpected given the extended reaction times and absence of the cognate TNA triphosphate in the reaction. The low polymerase activity is supported by molecular modeling, showing that the methyl groups of 4′-(*R*)- and 4′-(*S*)-Me-TNA result in unfavorable close contacts with the side chains of catalytic aspartates 541 and 543 in the active site of the polymerase (Figure 10). Additionally, the methyl group of the (*S*) isomer may clash with the 3′-terminal residue of the DNA primer. Together, these results suggest that the 10−92 TNA polymerase has a tight active site pocket that is incompatible with C4′-methyl substitution. As this polymerase, which selectively recognizes TNA, was inhibited by the 4′-Me-TNA triphosphates, it is unlikely that endogenous DNA and RNA polymerases will use these modified triphosphates as substrates.

Modeling Predicts 4′-Me-TNA Triphosphates to Be Poor Substrates for Mitochondrial Polymerase

We also evaluated the potential for use of the 4′-Me-TNA triphosphates by the mitochondrial polymerase γ (Polγ) based on the crystal structure of its ternary complex with dCTP. The modeling indicates steric conflicts due to a 4′-methyl group of either chirality from TNA-T triphosphates (tTTPs) that would preclude incorporation of a 4′-Me-TNA nucleotide (Figure 11).

■ CONCLUSIONS

siRNAs modified with TNA demonstrated that site-specific modification with TNA can increase potency, duration of action, and safety of these agents.[12] The TNA modification considerably improves stability of siRNAs under conditions mimicking acidic environment of endosomes for an extended period of time.[12] We had also previously observed that 2′ and 5′ methyl substituents on various RNA mimics modulate RNA interference activity in a manner that depends on chirality.[20,21] To combine the advantages of TNA and chiral substituent at the 4′ position, we synthesized 4′-(*R*)- and 4′-(*S*)-methyl TNA building blocks and evaluated the properties of oligonucleotides

Downloaded from pubs.acs.org/jacsat/article-pdf/148/36/38692/6822318/jacs.6c07051.pdf by VANDERBILT UNIV user on 10 October 2026

https://doi.org/10.1021/jacs.6c07051
J. Am. Chem. Soc. 2026, 148, 38692−38706

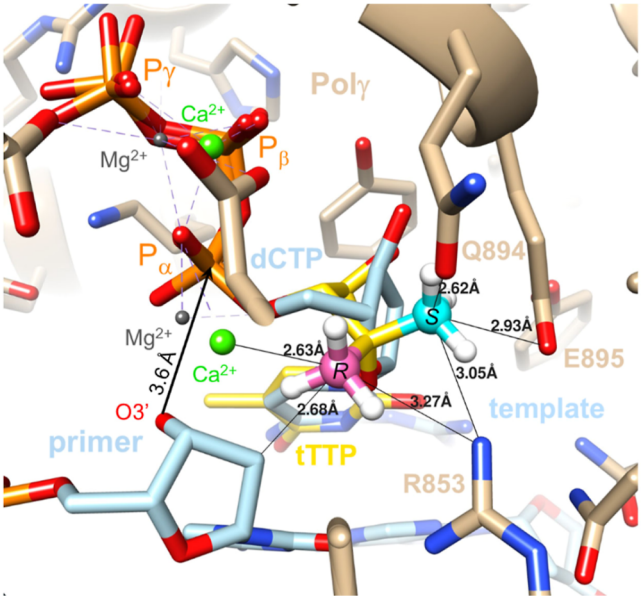


Figure 11. Mitochondrial Polγ is not expected to use 4′-Me-TNA triphosphates as substrates. The active site in the crystal structure of the ternary Polγ·DNA·dCTP Mg^{2+} complex (PDB ID 4ZTZ) is viewed via the minor groove of the template-primer duplex. tTTP (yellow carbon atoms) and two Ca^{2+} ions from the crystal structure of the ternary Pol*n*·DNA·tTTP Ca^{2+} complex (PDB ID 9CIQ)[34] were superimposed on the incoming dCTP and Mg^{2+}. The modeled 4′-(*R*)- (pink sphere) and 4′-(*S*)-methyl groups (cyan sphere) of the 4′-Me-TNA triphosphates are in steric conflict with metal ion, terminal primer residue, and various Polγ amino acid side chains. Short contacts and Mg^{2+} coordination spheres are indicated with thin solid and dashed lines, respectively, and the distance between O3′ of the 3′-terminal primer residue and P_a is shown with an arrow.

containing these modified residues. This position is an unexplored chemical space in TNA-based RNA therapeutics. Even small structural changes such as methyl substitution can profoundly influence pharmacokinetic and pharmacodynamic behavior of drug substances through chirality-dependent steric and conformational effects, a phenomenon often referred to as the "magic methyl" effect.[36,37] The 4′-Me-TNAs functionalized with A, G, C, U, and T nucleobases were synthesized from readily available carbohydrate precursors. As TNAs are known for their extreme nuclease resistance,[8] we evaluated the impact of terminal chiral 4′-Me-TNAs on the resistance of DNA oligonucleotides to exonuclease digestion. The 4′-Me-TNAs provided protection from 5′- and 3′-exonuclease-mediated degradation that is similar to that of the parent TNA. These biophysical properties were rationalized by analyses of the crystal structures of 4′-(*R*)-Me-TNA- and 4′-(*S*)-Me-TNA-containing oligonucleotides and molecular modeling using these structures in combination with structural data from nuclease crystal structures.

Like the parent TNA,[12] 4′-Me-TNAs thermodynamically destabilized an otherwise RNA duplex. The (*R*) isomer was more destabilizing than the (*S*) isomer. Strategic incorporation of modifications that destabilize RNA duplexes inhibit seed region-mediated off-target effects of siRNAs.[12] Thus, the altered hybridization properties of 4′-(*R*)-Me-TNA and 4′-(*S*)-Me-TNA may provide opportunities to tune target recognition and reduce off-target effects in RNAi applications.[12]

While it is well-known that another unnatural nucleic acid modification (*S*)-glycol nucleic acid, (*S*)-GNA, can reduce RNAi-mediated off-target effects[38] and is being evaluated successfully in many clinical studies of RNAi therapeutics, it has some structural limitations. The known flipped nucleobase orientation of GNA inside RNA is well-documented, and G:C pairs are not tolerated in RNA:(*S*)-GNA duplexes.[39,40] On the other hand, unlike GNA, TNA does not exhibit the flipped nucleobase orientation, and its right-handed backbone curvature, nucleobase orientation, and backbone-base inclination angle are similar to those of RNA. Because of these features, TNA pairs stably with itself, and it cross-pairs with both DNA and RNA,[1,41] and it is therefore worthwhile to explore its potential for mitigating off-target effects in RNAi.[12]

The 4′-(*R*)- and 4′-(*S*)-Me-TNA triphosphates are poor substrates of primer extension by the 10−92 TNA polymerase. Modeling revealed that the methyl groups of 4′-(*R*)- and 4′-(*S*)-Me-TNA are incompatible with the active site of this polymerase. This property may be advantageous from the perspective of therapeutic oligonucleotide design. Cellular toxicity associated with nucleotide analogs can arise when metabolites are recycled into DNA or RNA, leading to unintended effects on replication or transcription. Modeling of 4′-Me-TNA triphosphates within the active site of a mitochondrial polymerase further supports the hypothesis that these nucleotides are unlikely to be substrates for endogenous polymerases. Such a reduced likelihood of interaction with endogenous polymerase systems may lower the potential for genotoxicity.

It is important to note, however, that in this study we evaluated these two chiral Me-TNA modifications only against the engineered 10−92 TNA polymerase and found them to be poor substrates. The ability of mitochondrial and other endogenous polymerases to incorporate these modified nucleotides remains to be experimentally evaluated. Furthermore, nucleobase identity may also influence substrate recognition and incorporation efficiency by endogenous polymerases. Additional studies will therefore be required to fully assess the biological fate, metabolic processing, and safety profile of these modifications.

Although additional studies in animal models are beyond the scope of the present work, our data support the conclusion that 4′-Me-TNA nucleotides combine improved nuclease resistance, favorable conformational features for RNA targeting, and potential for off-target mitigation for RNAi with low apparent risk of polymerase-mediated safety issues. These desirable properties warrant further investigation of 4′-Me-TNA in the context of therapeutic oligonucleotide design. Furthermore, the 4′-position represents previously unexplored chemical space within TNA for RNA-based therapeutics, diagnostics, and related biochemical applications.

■ ASSOCIATED CONTENT

Data Availability Statement

Final coordinates and structure factors for the RNA crystal structures with incorporated 4′-(*R*)- and 4′-(*S*)-Me-TNA-T have been deposited in the Protein Data Bank https://www.rcsb.org/: PDB ID codes 9YRE and 9YRD, respectively.

Supporting Information

The Supporting Information is available free of charge at https://pubs.acs.org/doi/10.1021/jacs.6c07051.

Experimental details and general conditions, synthetic procedures and compound characterization of building blocks, synthetic procedures and compound character-

Downloaded from pubs.acs.org/jacsat/article-pdf/148/36/38692/6822318/jacs.6c07051.pdf by VANDERBILT UNIV user on 10 October 2026

https://doi.org/10.1021/jacs.6c07051
J. Am. Chem. Soc. 2026, 148, 38692−38706

ization of oligonucleotides, triphosphate syntheses and characterization, thermal melting temperatures, crystallization procedures, crystal data, data collection and refinement, polymerase recognition assay protocols, NMR spectra, and HPLC chromatograms (PDF)

AUTHOR INFORMATION

Corresponding Author

Muthiah Manoharan − *Alnylam Pharmaceuticals, Cambridge, Massachusetts 02142, United States;* orcid.org/0000-0002-7931-1172; Email: mmanoharan@alnylam.com

Authors

Atsushi Mikami − *Alnylam Pharmaceuticals, Cambridge, Massachusetts 02142, United States*

Dhrubajyoti Datta − *Alnylam Pharmaceuticals, Cambridge, Massachusetts 02142, United States;* orcid.org/0000-0003-2077-1294

Jayanta Kundu − *Alnylam Pharmaceuticals, Cambridge, Massachusetts 02142, United States;* orcid.org/0000-0003-2669-8112

Vathan Kumar − *Alnylam Pharmaceuticals, Cambridge, Massachusetts 02142, United States;* orcid.org/0000-0002-2837-419X

Namrata Erande − *Alnylam Pharmaceuticals, Cambridge, Massachusetts 02142, United States*

Esau Medina − *Department of Pharmaceutical Sciences, University of California, Irvine, California 92697-3958, United States*

Victoria A. Maola − *Department of Pharmaceutical Sciences, University of California, Irvine, California 92697-3958, United States*

Erica M. Lee − *Department of Pharmaceutical Sciences, University of California, Irvine, California 92697-3958, United States*

Shigeo Matsuda − *Alnylam Pharmaceuticals, Cambridge, Massachusetts 02142, United States*

Joel M. Harp − *Department of Biochemistry, Vanderbilt University, School of Medicine, Nashville, Tennessee 37232, United States*

Martin Egli − *Department of Biochemistry, Vanderbilt University, School of Medicine, Nashville, Tennessee 37232, United States;* orcid.org/0000-0003-4145-356X

John C. Chaput − *Department of Pharmaceutical Sciences, University of California, Irvine, California 92697-3958, United States;* orcid.org/0000-0003-1393-135X

Complete contact information is available at: https://pubs.acs.org/10.1021/jacs.6c07051

Notes

The authors declare no competing financial interest.

ACKNOWLEDGMENTS

We gratefully acknowledge Dr. Kevin Fitzgerald and the entire Research and Development organization for their unwavering guidance and support. We thank Drs. Mark K. Schlegel and Maja M. Janas for their significant contributions to RNAi off-target mitigation research at Alnylam. We are also grateful to Professor P. I. Pradeepkumar (Indian Institute of Technology, Bombay) for his valuable discussions and insights. We dedicate this manuscript to the legacy of Professor Albert Eschenmoser. We sincerely acknowledge Dr. Kevin Fitzgerald and the entire Research and Development organization for their guidance and support. We thank Drs. Mark K. Schlegel and Maja M. Janas for their pioneering contributions to RNAi off-target mitigation studies at Alnylam. We also thank Professor P. I. Pradeepkumar (IIT Bombay) for helpful discussions.

DEDICATION

We dedicate this manuscript to the memory of Professor Albert Eschenmoser, the inventor of TNA. We also honor the memory of Professor Fritz Eckstein, a pioneering chemist whose transformative contributions to oligonucleotide chemistry, particularly to the discovery and applications of phosphorothioate oligonucleotides, and to oligonucleotide therapeutics have left an indelible mark on the field. We dedicate this work to his extraordinary scientific legacy and cherished memory.

REFERENCES

(1) Schöning, K. U.; Scholz, P.; Guntha, S.; Wu, X.; Krishnamurthy, R.; Eschenmoser, A. Chemical etiology of nucleic acid structure: the α-threofuranosyl-(3′−2′) oligonucleotide system. *Science* **2000**, *290*, 1347−1351.

(2) Eschenmoser, A. Chemical etiology of nucleic acid structure. *Science* **1999**, *284*, 2118−2124.

(3) Yang, Y.-W.; Zhang, S.; McCullum, E. O.; Chaput, J. C. Experimental evidence that GNA and TNA were not sequential polymers in the prebiotic evolution of RNA. *J. Mol. Evol.* **2007**, *65*, 289−295.

(4) Lackey, H. H.; Peterson, E. M.; Chen, Z.; Harris, J. M.; Heemstra, J. M. Thermostability Trends of TNA:DNA Duplexes Reveal Strong Purine Dependence. *ACS Synth. Biol.* **2019**, *8*, 1144−1152.

(5) Ebert, M.-O.; Mang, C.; Krishnamurthy, R.; Eschenmoser, A.; Jaun, B. The structure of a TNA-TNA complex in solution: NMR study of the octamer duplex derived from α-(L)-threofuranosyl-(3′−2′)-CGAATTCG. *J. Am. Chem. Soc.* **2008**, *130*, 15105−15115.

(6) Wilds, C. J.; Wawrzak, Z.; Krishnamurthy, R.; Eschenmoser, A.; Egli, M. Crystal structure of a B-form DNA duplex containing (L)-α-threofuranosyl (3′−2′) nucleosides: a four-carbon sugar is easily accommodated into the backbone of DNA. *J. Am. Chem. Soc.* **2002**, *124*, 13716−13721.

(7) Pallan, P. S.; Wilds, C. J.; Wawrzak, Z.; Krishnamurthy, R.; Eschenmoser, A.; Egli, M. Why does TNA cross-pair more strongly with RNA than with DNA? An answer from X-ray analysis. *Angew. Chem., Int. Ed.* **2003**, *42*, 5893−5895.

(8) Culbertson, M. C.; Temburnikar, K. W.; Sau, S. P.; Liao, J.-Y.; Bala, S.; Chaput, J. C. Evaluating TNA stability under simulated physiological conditions. *Bioorg. Med. Chem. Lett.* **2016**, *26*, 2418−2421.

(9) Lee, E. M.; Setterholm, N. A.; Hajjar, M.; Barpuzary, B.; Chaput, J. C. Stability and mechanism of threose nucleic acid toward acid-mediated degradation. *Nucleic Acids Res.* **2023**, *51*, 9542−9551.

(10) Chaput, J. C. Redesigning the Genetic Polymers of Life. *Acc. Chem. Res.* **2021**, *54*, 1056−1065.

(11) Anosova, I.; Kowal, E. A.; Dunn, M. R.; Chaput, J. C.; Van Horn, W. D.; Egli, M. The structural diversity of artificial genetic polymers. *Nucleic Acids Res.* **2016**, *44*, 1007−1021.

(12) Matsuda, S.; Bala, S.; Liao, J. Y.; Datta, D.; Mikami, A.; Woods, L.; Harp, J. M.; Gilbert, J. A.; Bisbe, A.; Manoharan, R. M.; et al. Shorter Is Better: The α-(L)-Threofuranosyl Nucleic Acid Modification Improves Stability, Potency, Safety, and Ago2 Binding and Mitigates Off-Target Effects of Small Interfering RNAs. *J. Am. Chem. Soc.* **2023**, *145*, 19691−19706.

(13) Wang, F.; Liu, L. S.; Li, P.; Lau, C. H.; Leung, H. M.; Chin, Y. R.; Tin, C.; Lo, P. K. Cellular uptake, tissue penetration, biodistribution, and biosafety of threose nucleic acids: Assessing in vitro and in vivo delivery. *Mater. Today Bio* **2022**, *15*, 100299.

(14) Lozoya-Colinas, A.; Yu, Y.; Chaput, J. C. Functionally Enhanced XNA Aptamers Discovered by Parallelized Library Screening. *J. Am. Chem. Soc.* **2023**, *145*, 25789−25796.

Downloaded from pubs.acs.org/jacsat/article-pdf/148/36/38692/6822318/jacs.6c07051.pdf by VANDERBILT UNIV user on 10 October 2026

(15) Yu, H.; Zhang, S.; Chaput, J. C. Darwinian evolution of an alternative genetic system provides support for TNA as an RNA progenitor. *Nat. Chem.* **2012**, *4*, 183−187.
(16) Wang, Y.; Wang, Y.; Song, D.; Sun, X.; Zhang, Z.; Li, X.; Li, Z.; Yu, H. A Threose Nucleic Acid Enzyme with RNA Ligase Activity. *J. Am. Chem. Soc.* **2021**, *143*, 8154−8163.
(17) Nikoomanzar, A.; Chim, N.; Yik, E. J.; Chaput, J. C. Engineering polymerases for applications in synthetic biology. *Q. Rev. Biophys.* **2020**, *53*, No. e8.
(18) Larsen, A. C.; Dunn, M. R.; Hatch, A.; Sau, S. P.; Youngbull, C.; Chaput, J. C. A general strategy for expanding polymerase function by droplet microfluidics. *Nat. Commun.* **2016**, *7*, 11235.
(19) Lu, X.; Wu, X.; Wu, T.; Han, L.; Liu, J.; Ding, B. Efficient construction of a stable linear gene based on a TNA loop modified primer pair for gene delivery. *Chem. Commun.* **2020**, *56*, 9894−9897.
(20) Mikami, A.; Erande, N.; Matsuda, S.; Kel'in, A.; Woods, L. B.; Chickering, T.; Pallan, P. S.; Schlegel, M. K.; Zlatev, I.; Egli, M.; et al. Synthesis, chirality-dependent conformational and biological properties of siRNAs containing 5′-(R)- and 5′-(S)-C-methyl-guanosine. *Nucleic Acids Res.* **2020**, *48*, 10101−10124.
(21) Guenther, D. C.; Mori, S.; Matsuda, S.; Gilbert, J. A.; Willoughby, J. L. S.; Hyde, S.; Bisbe, A.; Jiang, Y.; Agarwal, S.; Madaoui, M.; et al. Role of a "Magic" Methyl: 2′-Deoxy-2′-α-F-2′-β-C-methyl Pyrimidine Nucleotides Modulate RNA Interference Activity through Synergy with 5′-Phosphate Mimics and Mitigation of Off-Target Effects. *J. Am. Chem. Soc.* **2022**, *144*, 14517−14534.
(22) Dahlman, O.; Garegg, P. J.; Mayer, H.; Schramek, S.; Krogsgaard-Larsen, P.; Ryhage, R.; Isaksson, R. Synthesis of three 3-C-hydroxymethylpentoses with the D-ribo-D-xylo- and L-lyxo-configurations. Identification of the latter with a monosaccharide isolated from phase I Coxiella burnetii lipopolysaccharide. *Acta Chem. Scand. B* **1986**, *40*, 15−20.
(23) Varada, M.; Aher, M.; Erande, N.; Kumar, V. A.; Fernandes, M. Methoxymethyl Threofuranosyl Thymidine (4'-MOM-TNA-T) at the T7 Position of the Thrombin-Binding Aptamer Boosts Anticoagulation Activity, Thermal Stability, and Nuclease Resistance. *ACS Omega* **2020**, *5*, 498−506.
(24) Wen, J.; Zhang, C.; Chen, X.; Dai, Z.; Li, M.; Ma, W.; Yam, C.; Huang, X.; Xiong, C.; Mei, H. An epimer of threose nucleic acid enhances oligonucleotide exonuclease resistance through end capping. *Commun. Chem.* **2025**, *8*, 144.
(25) Sun, J.; Dou, Y.; Ding, H.; Yang, R.; Sun, Q.; Xiao, Q. First Total Synthesis of a Naturally Occurring Iodinated 5′-Deoxyxylofuranosyl Marine Nucleoside. *Mar. Drugs* **2012**, *10*, 881−889.
(26) Zlatev, I.; Manoharan, M.; Vasseur, J.-J.; Morvan, F. Solid-Phase Chemical Synthesis of 5′-Triphosphate DNA, RNA, and Chemically Modified Oligonucleotides. *Curr. Protoc. Nucleic Acid Chem.* **2012**, *50*, 1.28.1.
(27) Zhang, S.; Yu, H.; Chaput, J. C. Synthesis of Threose Nucleic Acid (TNA) Triphosphates and Oligonucleotides by Polymerase-Mediated Primer Extension. *Curr. Protoc. Nucleic Acid Chem.* **2013**, *52*, 4.54.1.
(28) Brautigam, C. A.; Steitz, T. A. Structural principles for the inhibition of the 3′-5′ exonuclease activity of Escherichia coli DNA polymerase I by phosphorothioates. *J. Mol. Biol.* **1998**, *277*, 363−377.
(29) Jinek, M.; Coyle, S. M.; Doudna, J. A. Coupled 5′ nucleotide recognition and processivity in Xrn1-mediated mRNA decay. *Mol. Cell* **2011**, *41*, 600−608.
(30) Pettersen, E. F.; Goddard, T. D.; Huang, C. C.; Couch, G. S.; Greenblatt, D. M.; Meng, E. C.; Ferrin, T. E. UCSF Chimera—a visualization system for exploratory research and analysis. *J. Comput. Chem.* **2004**, *25*, 1605−1612.
(31) Case, D. A.; Cheatham, T. E., 3rd.; Darden, T.; Gohlke, H.; Luo, R.; Merz, K. M., Jr.; Onufriev, A.; Simmerling, C.; Wang, B.; Woods, R. J. The Amber biomolecular simulation programs. *J. Comput. Chem.* **2005**, *26*, 1668−1688.
(32) Muniz, M. I.; Lackey, H. H.; Heemstra, J. M.; Weber, G. DNA/TNA mesoscopic modeling of melting temperatures suggests weaker hydrogen bonding of CG than in DNA/RNA. *Chem. Phys. Lett.* **2020**, *749*, 137413.
(33) Reynders, S.; Rihon, J.; Lescrinier, E. Molecular Modeling on Duplexes with Threose-Based TNA and TPhoNA Reveals Structural Basis for Different Hybridization Affinity toward Complementary Natural Nucleic Acids. *J. Chem. Theory Comput.* **2025**, *21*, 2798−2814.
(34) Tomar, R.; Ghodke, P. P.; Patra, A.; Smyth, E.; Pontarelli, A.; Copp, W.; Guengerich, F. P.; Chaput, J. C.; Wilds, C. J.; Stone, M. P.; et al. DNA Replication across α-L-(3′−2′)-Threofuranosyl Nucleotides Mediated by Human DNA Polymerase η. *Biochemistry* **2024**, *63*, 2425−2439.
(35) Maola, V. A.; Yik, E. J.; Hajjar, M.; Lee, J. J.; Holguin, M. J.; Quijano, R. N.; Nguyen, K. K.; Ho, K. L.; Medina, J. V.; Chim, N.; et al. Directed evolution of a highly efficient TNA polymerase achieved by homologous recombination. *Nat. Catal.* **2024**, *7* (11), 1173−1185.
(36) Barreiro, E. J.; Kümmerle, A. E.; Fraga, C. A. M. The Methylation Effect in Medicinal Chemistry. *Chem. Rev.* **2011**, *111*, 5215−5246.
(37) Pinheiro, P. S. M.; Franco, L. S.; Fraga, C. A. M. The Magic Methyl and Its Tricks in Drug Discovery and Development. *Pharmaceuticals* **2023**, *16*, 1157.
(38) Janas, M. M.; Schlegel, M. K.; Harbison, C. E.; Yilmaz, V. O.; Jiang, Y.; Parmar, R.; Zlatev, I.; Castoreno, A.; Xu, H.; Shulga-Morskaya, S.; et al. Selection of GalNAc-conjugated siRNAs with limited off-target-driven rat hepatotoxicity. *Nat. Commun.* **2018**, *9*, 723.
(39) Schlegel, M. K.; Matsuda, S.; Brown, C. R.; Harp, J. M.; Barry, J. D.; Berman, D.; Castoreno, A.; Schofield, S.; Szeto, J.; Manoharan, M.; et al. Overcoming GNA/RNA base-pairing limitations using iso-nucleotides improves the pharmacodynamic activity of ESC+ GalNAc-siRNAs. *Nucleic Acids Res.* **2021**, *49*, 10851−10867.
(40) Schlegel, M. K.; Janas, M. M.; Jiang, Y.; Barry, J. D.; Davis, W.; Agarwal, S.; Berman, D.; Brown, C. R.; Castoreno, A.; LeBlanc, S.; et al. From bench to bedside: Improving the clinical safety of GalNAc-siRNA conjugates using seed-pairing destabilization. *Nucleic Acids Res.* **2022**, *50*, 6656−6670.
(41) Egli, M.; Schlegel, M. K.; Manoharan, M. Acyclic (S)-glycol nucleic acid (S-GNA) modification of siRNAs improves the safety of RNAi therapeutics while maintaining potency. *RNA* **2023**, *29*, 402−414.

Downloaded from pubs.acs.org/jacsat/article-pdf/148/36/38692/6822188/jacs.6c07051.pdf by VANDERBILT UNIV user on 10 October 2026

https://doi.org/10.1021/jacs.6c07051
J. Am. Chem. Soc. 2026, 148, 38692−38706